J. Biochem. **142,** 517–524 (2007)
doi:10.1093/jb/mvm158

Structural Evidence for Endocrine Disruptor Bisphenol A Binding to Human Nuclear Receptor ERRγ

Ayami Matsushima[1], Yoshimitsu Kakuta[2], Takamasa Teramoto[2], Takumi Koshiba[3], Xiaohui Liu[1], Hiroyuki Okada[1], Takatoshi Tokunaga[1], Shun-ichiro Kawabata[3], Makoto Kimura[2] and Yasuyuki Shimohigashi[1,*]

[1]Laboratory of Structure-Function Biochemistry, Department of Chemistry, Research-Education Centre of Risk Science, Faculty and Graduate School of Sciences; [2]Laboratory of Biochemistry, Department of Agricultural Chemistry, Faculty and Graduate School of Agriculture; and [3]Laboratory of Life Biochemistry, Department of Biological Science, Faculty of Sciences, Kyushu University, Fukuoka 812-8581, Japan

Received May 30, 2007; accepted July 25, 2007; published online August 30, 2007

Many lines of evidence reveal that bisphenol A (BPA) functions at very low doses as an endocrine disruptor. The human estrogen-related receptor γ (ERRγ) behaves as a constitutive activator of transcription, although the endogenous ligand is unknown. We have recently demonstrated that BPA binds strongly to ERRγ (K_D = 5.5 nM), but not to the estrogen receptor (ER). BPA preserves the ERRγ's basal constitutive activity, and protects the selective ER modulator 4-hydroxytamoxifen from its deactivation of ERRγ. In order to shed light on a molecular mechanism, we carried out the X-ray analysis of crystal structure of the ERRγ ligand-binding domain (LBD) complexed with BPA. BPA binds to the receptor cavity without changing any internal structures of the pocket of the ERRγ-LBD apo form. The hydrogen bonds of two phenol-hydroxyl groups, one with both Glu275 and Arg316, the other with Asn346, anchor BPA in the pocket, and surrounding hydrophobic bonds, especially with Tyr326, complete BPA's strong binding. Maintaining the 'activation helix' (helix 12) in an active conformation would as a result preserve receptor constitutive activity. Our results present the first evidence that the nuclear receptor forms complexes with the endocrine disruptor, providing detailed molecular insight into the interaction features.

Key words: binding assay, bisphenol A, estrogen-related receptor γ (ERRγ), nuclear receptor, X-ray crystal structure.

Abbreviations: BPA, bisphenol A; CBB, Coomassie brilliant blue; CHAPS, 3-[3-(cholamidopropyl)dimethylammonio]-1-propanesulfonic acid; DES, diethylstilbestrol; ER, estrogen receptor; ERR, estrogen-related receptor; ERE, estrogen response element; ERRE, ERR-response element; LBD, ligand-binding domain; MALDI-TOF, matrix-assisted laser desorption ionization time-of-flight; NR, nuclear receptor; 4-OHT, 4-hydroxytamoxifen; and PCR, polymerase chain reaction.

Bisphenol A (BPA), 2,2-bis(4-hydroxyphenyl)propane, has a symmetrical chemical structure of HO-C_6H_4-$C(CH_3)_2$-C_6H_4-OH. BPA is used mainly in the production of polycarbonate plastics and epoxy resins. Its worldwide manufacture is ~3.2 million metric tons per year. BPA had been acknowledged as an estrogenic chemical able to interact with human estrogen receptors (ERs) (*1*, *2*). In recent years, many lines of evidence reveal that BPA functions at its very low doses as an endocrine disruptor (*3*–*7*).

All of these so-called 'low-dose effects' of BPA have been explained as the output effects of steroid hormone receptor ERs (*8*). However, since BPA's binding to ER and hormonal activity is extremely weak, 1,000–10,000 times lower than for natural hormones, the intrinsic significance of low-dose effects has been intangible and obscure. BPA's low-dose effects have been peer-reviewed by the National Toxicology Program of the United States (*9*), and extensively reviewed by vom Saal and Hughes (*7*). The discrepancy on low-dose effects prompted us to enquire whether BPA may interact with nuclear receptors (NRs) other than ER, and as a BPA receptor we have recently identified the human estrogen-related receptor γ (ERRγ) (*10*).

The ERRγ belongs to the orphan subfamily of NRs (*11*), all members of which (ERRα, ERRβ and ERRγ) are closely related to ERs (*12*, *13*). ERRγ behaves as a constitutive activator of transcription, presumably with intrinsic roles in differentiation and maturation of the foetal brain. Although the endogenous ligand is unknown, we have shown that BPA binds strongly to ERRγ, but not to ER (*10*). BPA preserves the ERRγ's basal constitutive activity, and protects the selective ER modulator 4-hydroxytamoxifen (4-OHT) from its deactivation of ERRγ.

In order to explain such BPA's activities at the structural basis, we carried out the crystallization of the ERRγ ligand-binding domain (LBD) complexed with BPA. We here report the structure of the complex and shed light on a molecular mechanism between BPA and

*To whom correspondence should be addressed. Tel: +81-92-642-2584; Fax: +81-92-642-2584;
E-mail: shimoscc@mbox.nc.kyushu-u.ac.jp

ERRγ-LBD. This is the first straight evidence that the nuclear receptor forms a complex with the endocrine disruptor BPA. In the interaction with the receptor ERRγ, BPA was demonstrated to act as an inverse antagonist against 4-OHT's inverse agonist activity.

MATERIALS AND METHODS

Materials—3-[3-(Cholamidopropyl)dimethylammonio]-1-propanesulfonic acid (CHAPS), EDTA, HEPES and γ-globulin were obtained from Sigma (St Louis, MO, USA). Glycerol was from Nacalai Tesque (Kyoto), and all other chemicals used were of analytical grade and purchased from Wako (Osaka).

Methods—The concentration of nuclear receptor protein was estimated by the Bradford method (*14*) using the protein assay solution with Coomassie brilliant blue (CBB) (Nacalai Tesque). Mass spectra of proteins were measured on a mass spectrometer Voyager™ DE-PRO (PerSeptive Biosystems Inc., Framingham, MA, USA) using the matrix-assisted laser desorption ionization time-of-flight (MALDI-TOF) method.

Construction of Recombinant Plasmid—The cDNA fragment encoding human ERRγ-LBD (corresponding to amino acid residues 222–458) were generated by polymerase chain reaction (PCR) from kidney QUICK-Clone™ cDNA (Clonetech, Mountain View, CA, USA) using specific primers. The amplified product was cloned into the expression vector pGEX 6P-1 (Amersham Biosciences, Piscataway, NJ, USA) using *Eco*RI and *Xho*I restriction enzyme sites to express the product as a glutathione *S*-transferase (GST) fusion protein.

Site-directed Mutagenesis of ERRγ—The constructed plasmid were served as a template for Ala-substituted mutants. The PCR method was carried out to introduce the single-point mutations by using a series of overlapping sense and antisense primer pairs. The PCR fragments containing the E275A, M306A, L309A, R316A, Y326A, N346A and F435A mutations were cut with *Eco*RI and *Xho*I, and then subcloned into the expressing vector pGEX 6P-1.

Saturation Binding Assay—Saturation binding assay was conducted essentially as reported (*15*) at 4°C overnight to minimize degradation of the ligand receptor complex in a final volume of 100 μl of binding buffer [10 mM HEPES (pH 7.5), 50 mM NaCl, 2 mM $MgCl_2$, 1 mM EDTA, 2 mM CHAPS and 2 mg/ml γ-globulin]. GST-ERRγ-LBD of 30–3000 ng and [^{3}H]BPA (185 GBq/mmol, America Radiolabeled Chemicals Inc., St Louis, MO, USA) with or without addition of unlabelled BPA (final concentration of 10 μM) to quantify the non-specific binding. Free radio-ligand was removed by centrifugation (4°C, 10 min, 14,000 r.p.m.) or filtration after incubation with 100 μl of 1% dextran-coated charcoal (Sigma, St Louis, MO, USA) in PBS (pH 7.4) for 10 min at 4°C. Specific binding of [^{3}H]BPA was calculated by subtracting the non-specific binding from the total binding.

Protein Expression and Purification—GST fusion protein of the ERRγ-LBD was expressed by using *Escherichia coli* BL21 as described previously (*10*). Purification was carried out by using an affinity column of glutathione-sepharose 4B (Amersham Biosciences). GST was cleaved on the resin by using a specific enzyme, PreScission Protease (Amersham Biosciences), for 4 h at 4°C. After incubation, ERRγ-LBD was eluted and its concentration determined by the Bradford method using a CBB solution (*14*).

Crystallization of Protein Complex Followed by X-Ray Data Collection and Processing—Purified ERRγ-LBD was concentrated by ultrafiltration. Co-crystallization with a 3-fold molar excess of BPA was carried out with the hanging drop vapour diffusion method. The crystals used for data collection were from a drop of 2 μl of ERRγ-LBD solution mixed with BPA and 2 μl of reservoir solution (50 mM HEPES pH 7.5, 0.75 M sodium citrate and 5% glycerol). For data collection, crystals were transferred into a cryoprotectant solution containing 24% glycerol in reservoir solution, then mounted in a nylon loop and flash-frozen in a nitrogen stream at 100 K. X-ray diffraction data were collected at the beamline BL38B1, SPring-8 (Hyogo, Japan). The data were integrated and scaled using the HKL*2000* package (*16*).

Structure Determination and Refinement—A monomer model of ERRγ-LBD/4-OHT (1S9Q) was used as a search molecule for molecular replacement using MOLREP (*17*) in CCP4 (*18*). The position of the monomer in the asymmetric unit was located and the structure refined at 1.6 Å using REFMAC5 (*19*) in CCP4. Manual adjustment and rebuilding of the model including BPA and water molecules were performed using the program Coot (*20*). The final model contained residues 232–458 of ERRγ, one BPA, three glycerol and 387 water molecules. Multiple conformers were applied to Lys236, Ser239, Ile249, Tyr250, Val278, Lys284, Ser290, Met298, Ser303, Ser319, Ser358, Ile382, Gln389, Asp393, Gln400, Asp401, Gln406, His407, Met419, Ser428, Gln433 and Leu454. The final model was validated with PROCHECK (*21*). Date collection and structure refinement statistics are summarized in Table 1.

Minimum-energy Calculations—For the energy calculations of the geometry optimization of BPA, the conventional Hartree–Fock (HF) method was used on a computer program Gaussian (v. 03) with the 6-31G(d, p) basis set.

RESULTS AND DISCUSSION

Dimeric Structure of ERRγ-LBD—The crystals usable for data collection were obtained from a ERRγ-LBD solution mixed with BPA in the following reservoir solution: 50 mM HEPES pH 7.5, 0.75 M sodium citrate and 5% glycerol. We solved the crystal structure of the resulting ERRγ-LBD in a complex with BPA at a resolution of 1.6 Å (space group $P4_12_12$) (Table 1). The ERRγ-LBD crystallized in homodimeric form using crystallographic 2-fold symmetry, indicating that BPA binding does not interfere with homodimer formation (Fig. 1A). Homodimer formation of the purified ERRγ-LBD is also observed by MALDI-TOF mass spectrometry (Fig. 2), in agreement with the reported homodimeric binding of ERRs to DNA (*22*). A BPA molecule in the complex with ERRγ-LBD is defined very well from its electron density (Fig. 1B).

Table 1. **Data collection and refinement statistics for X-ray crystal analysis of the ERRγ. LBD complexed with BPA.**

Data set	
Space group	$P4_12_12$
Unit cell parameters	$a = 64.05$ Å
	$b = 64.05$ Å
	$c = 136.87$
Data collection	
Beam line	SPring-8 BL38B1
Wavelength (Å)	1.0
Resolution range (Å)	28.06–1.60
Number of reflections	
Observed	433–326
Unique	36;414
R_{sym}[a,b]	0.058 (0.349)
I/σ (I)[a]	40.4 (8.2)
Completeness (%)	99.6
Refinement statistics	
Resolution range (Å)	28.06–1.60
Number of reflections	36,414
Working set	34,493
Test set	1,921
Completeness (%)	99.6
R_{cryst}[c] (%)	16.9
R_{free}[d] (%)	19.7
Root mean square deviations	
Bond length (Å)	0.012
Bond angles (°)	1.333
Average B-factor (Å^2)	
Protein	18.9
BPA	15.5
Glycerol	39.1
Water	35.3
Number of atoms	2,357
Protein	1,935
BPA	17
Glycerol	18
Water	387
Ramachandran analysis	
Most favoured (%)	94.8
Allowed (%)	5.2
Generously allowed (%)	0.0
Disallowed (%)	0.0

[a]Values in parentheses are for the highest resolution shell. [b]$R_{sym} = \sum(-\langle I\rangle)/\sum\langle I\rangle$, where I is the intensity measurement for a given reflaction and $\langle I\rangle$ is the average intensity for multiple measurements of this reflaction. [c]$R_{cryst} = \sum|F_{obs} - F_{cal}|\sum F_{obs}$, where F_{obs} and F_{cal} are observed and calculated structure factor amplitudes. [d]R_{free} value was calculated for R_{cryst}, using only an undefined subset of reflection data (5%).

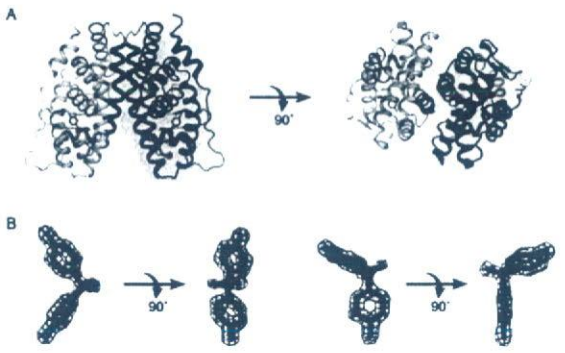

Fig. 1. **BPA/ERRγ-LBD complex.** (A) The panoramic view of whole-sphere BPA/ERRγ-LBD homodimer complex. Each panel shows the 3D-structure pictured from the top with 90° rotation. One molecule of BPA is in each ERRγ-LBD. BPA is shown in red colour. Characteristic α-helices are shown in distinctive colours; *i.e.* H10 in a dimerization interface, blue; H12 in an activation conformation, purple. (B) BPA bound to the ERRγ-LBD fitted into omitted Fo–Fc electron density maps at a level of 4.0 sigma. Right-side two panels show the aromatic face of BPA-A ring in a 90° rotation. Left-side two panels show the whole figure of the BPA molecule in a 90° rotation.

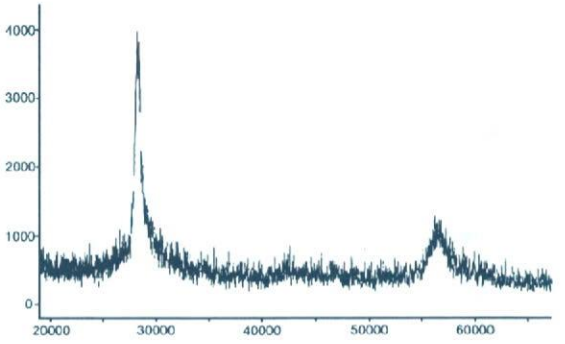

Fig. 2. **Dimer formation detected by MALDI-TOF mass spectrometry.** The peak of monomer emerges around 27,600 (calculated mass number [MH$^+$] of ERRγ-LBD: 27578.67), while the dimer peak is found at around 55,200.

ERRγ binds to the ERR-response element (ERRE), but as a monomer. ERRγ can also bind to functional estrogen response elements (EREs) in ER target genes, suggesting a possible overlap between ERR and ER action (*12*). Homodimers formed by the hydrophobic interactions between the interfaces of α-helix 10 (H10), which is supported by α-helix 7 (H7). Thus, in a homodimer, four α-helices are arranged in tandem to form the sequence H7–H10–H10–H7 (Fig. 1A, right). In the dimerization interface of H10–H10, such amino acid pairs as Pro422–*Pro422*, Arg425–*Gln426* and Gln426–*Arg425* appear to make a specific intermolecular interaction (Fig. 3A; the residues in italic characters are of the second molecule of ERRγ dimer). At the interface between H7 and H10, Tyr356–Thr420 and Met359–Met417 pairs are likely to underlie the intramolecular interaction (Fig. 3B). Leu418 and Leu421 in H10 are oriented towards the centre of the ERRγ-LBD and are conserved among almost all the NRs. In addition, almost all NRs conserve Leu399 in H9, and this Leu399 together with Leu418 and Leu421 in H10 take part in forming a hydrophobic core, which probably plays an intrinsic role in structural construction for homodimerization (Fig. 3C).

Binding Site of Bisphenol A—The binding site of BPA is constructed by a series of amino acid residues.

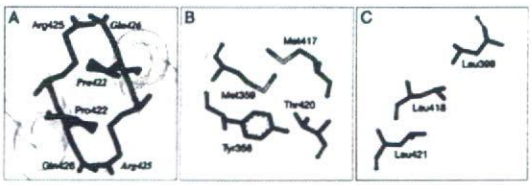

Fig. 3. **Intermolecular and intramolecular interactions of ERRγ-LBD.** (A) Dimer interface between H10 (blue) and *H10 (in the second molecule shown in italics)* is formed for amino acid residues such as Pro422–*Pro422*, Arg425–*Gln426*, and Gln426–*Arg425*. (B) Intramolecuar interaction between H7 (magenta) and H10 (blue) is seen for Tyr356 and Thr420, and for Met359 and Met417. (C) Highly conserved amino acid residues, Leu399 in H9, Leu418 and Leu421 in H10, are constructing a hydrophobic core.

Those in a range of 5 Å include Leu268, Cys269, Leu271, Ala272, Glu275 from H3; Trp305, Met306, Leu309, Val313, Arg316 from H5; Tyr326 from β-strand 1 (S1); Leu342, Leu345, Asn346, Ile349 from H7; Phe435 from H11 and Phe450 from H12 (Fig. 4A). In the BPA molecule, the two C_6H_4–OH (phenol) groups bind to the sp^3 carbon atom (sp^3-C) together with the two CH_3 groups, and thus their benzene-carbons adjacent to sp^3-C are arranged at the vertexes in a regular tetrahedron (Fig. 4B). It should be noted that BPA in the ERRγ-LBD complex is superimposed almost completely with BPA in the minimum-energy conformation (Fig. 4B). This demonstrates that BPA is present in the ERRγ-LBD binding pocket without any steric hindrance. Thus, BPA's phenol-hydroxyl oxygen atoms, C_6H_4–**O**H, are placed with a bond angle (O–sp^3–C–O) of about 105°, and are arranged to cross-link between Glu275/Arg316 and Asn346.

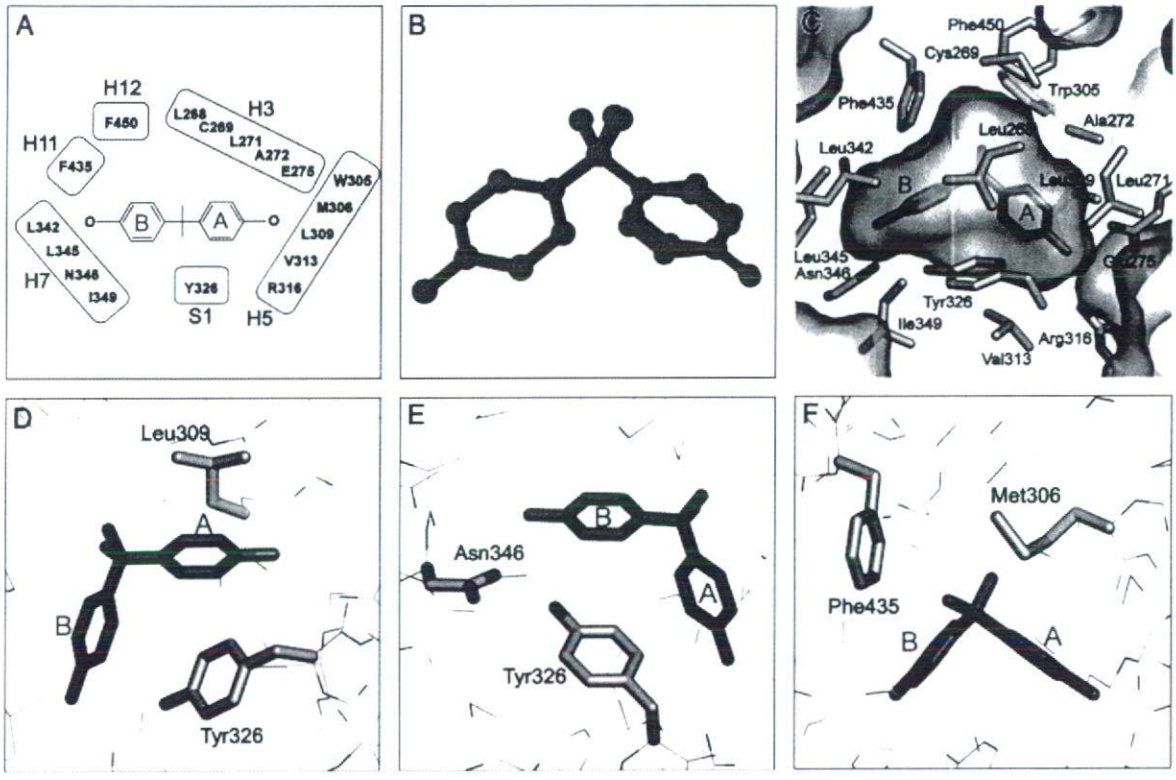

Fig. 4. **Identification of the binding sites of BPA in ERRγ-LBD.** (A) Schematic line-up of amino acid residues that form the LBP in ERRγ. The residues shown are in close proximity to BPA within 5 Å. (B) Superimposition of BPA (magenta) in the ERRγ-LBD complex and BPA (green) in the minimum-energy conformation calculated. They are almost completely overlaid, indicating that BPA fits the binding pocket of ERRγ-LBD without any conformational constrictions. The minimum-energy conformation was calculated and depicted by the conventional Hartree–Fock method using the computer program Gaussian (v. 03). (C) View of BPA in the cavity of ERRγ-LBD. The hydroxy groups of BPA's phenol-A and phenol-B rings are arranged to cross-link between Glu275/Arg316 and Asn346, respectively. (D) The BPA's A-ring is sandwiched with Leu309 and Tyr326 by characteristic hydrophobic interactions. The π face of A-ring interacts with the Leu309 isobutyl-methyl group, and the opposite π face of the same A-ring makes the T-shaped π/π interaction with Tyr326's phenol-benzene ring. (E) The BPA's B-ring is in a hydrogen bond with the Tyr326-phenol hydroxyl group. This OH/π bond appears to be a strong diving force to tether BPA in the ERRγ-LBP, together with the hydrogen bond between B-ring's hydroxy group and Asn346-β-carbonyl. (F) One of the CH_3 groups on the BPA's sp^3-C atom faces to Phe435 (H11) in a distance of 3.7 Å and another CH_3 group faces to the Met306 sulphur atom in a distance of 3.6 Å.

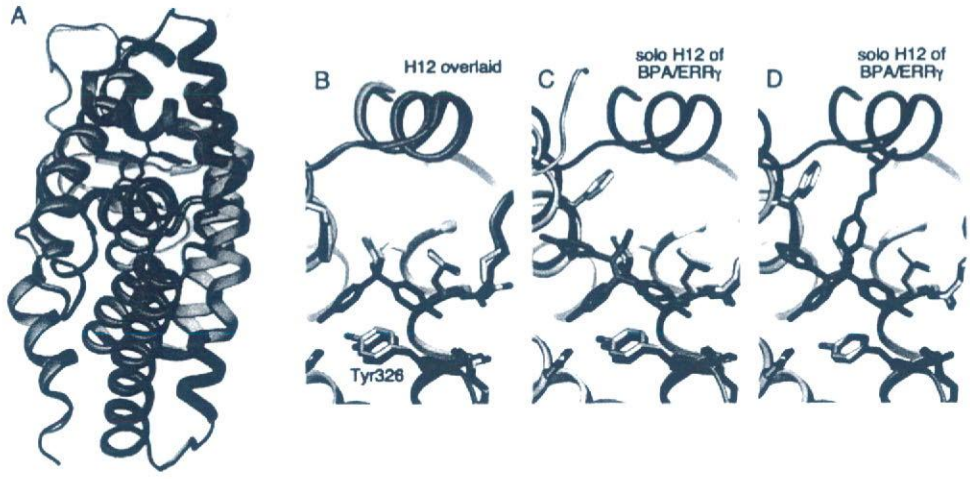

Fig. 5. **Superimposition of BPA or ERRγ-LBD and other ERRγ-LBD complexes.** (A) Superimposition of the whole LBD of BPA/ERRγ-LBD complex (blue) and the ERRγ-LBD apo form (grey) (1TFC; PDB code) (23). (B) The LBP of superimposed BPA/ERRγ-LBD complex (blue) and the ERRγ-LBD apo form (grey) (1TFC). The Tyr326-phenol groups are in a shift of about 10°, Tyr326-phenol of the BPA complex being underneath that of the apo form. (C) Superimposition of BPA/ERRγ-LBD complex (blue) and the DES/ERRγ-LBD complex (yellow) (1S9P) (23). The Tyr326-phenol groups are also in a slight shift. (D) Superimposition of the BPA/ERRγ-LBD complex (blue) and the 4-OHT/ERRγ-LBD (light blue) (1S9Q) (23). Superimposition of BPA (red) with DES (green) or 4-OHT (cyan) is carried out for α-helices to be overlaid. H12 in the BPA/ERRγ-LBD complex are shown in purple in all figures. H12 in the DES/ERRγ-LBD complex and in the 4-OHT/ERRγ-LBD complex are widely separated from a position in the activation conformation, and thus those are out of superimpositions between the BPA/ERRγ-LBD and the DES/ERRγ-LBD and 4-OHT/ERRγ-LBD complexes (C and D, respectively).

One of the two phenol-hydroxyl groups of BPA is anchored by hydrogen bonds with Glu275 (H3) and Arg316 (H5) at the one side of the ligand-binding pocket (LBP), while another hydroxyl group makes a hydrogen bond with Asn346 in H7 at the other side (Fig. 4C). Thus, BPA cross-links the residues Glu275/Arg316 and Asn346 with three hydrogen bonds. This is in stark contrast to the fact that diethylstilbestrol (DES) cross-links Glu275/Arg316 and His434 in H11 on the other side of the cavity (*23*). BPA's phenol-hydroxyl groups are not far enough apart to bridge between these Glu275/Arg316 and His434.

Key Amino Acid Tyr326 for Binding of Bisphenol A—Asn346 (H7) has been reported to interact with Tyr326 in S1 through a hydrogen bond (*23*, *24*). This hydrogen bond is also maintained in the BPA/ERRγ-LBD complex. In particular, we found that Tyr326 in the complex becomes the chief amino acid residue for BPA to be placed in the ERRγ-LBP, providing an appropriate and fitting space to pack BPA, having two phenol groups and two methyl groups. More importantly, Tyr326 interacts directly with BPA. The phenol group of the Tyr326 side chain keeps BPA's phenol-benzene rings A and B in the pocket by two strong interactions; i.e. by the hydrophobic *edge*-to-*face*-type, or T-shaped π/π interaction with BPA's benzene ring A, and by the OH/π interaction with BPA's benzene ring B (Fig. 4D and E). The Tyr-phenol benzene ring is able to make T-shaped π/π interactions with the aromatic side chains of amino acids such as Phe, Tyr, His and Trp (*25*, *26*). When one of six edges or vertexes of the benzene ring directs towards the π face of the counterpart aromatic ring, it makes so-called T-shaped π/π interaction(s). As seen in Fig. 4D, Tyr326's benzene ring indeed make a T-shaped π/π interaction with BPA's benzene ring A.

It should be noted that, at another π face on the opposite side, BPA's A ring interacts further with the Leu309 isobutyl-methyl groups (Fig. 4D). This interaction is also classified as a CH/π-type hydrophobic interaction. Consequently, there is a fascinating formation of sandwiched hydrophobic interactions of the A ring with Leu309 and Tyr326 (Fig. 4D). This is definitely a powerful driving force holding BPA in the LBD of ERRγ.

The Tyr326-phenol hydroxyl group makes another important interaction with BPA's benzene ring B. As shown in Fig. 4E, these are an OH/π interaction (*27*, *28*). OH/π interactions are one of the strongest interactions between amino acid side-chains (*25*, *26*). As a result, BPA's phenol B is tethered in the ERRγ-LBP complex by two essential interactions, the hydrogen bond with Asn346 and the OH/π bond with Tyr326.

It is noteworthy that Tyr326 has multiple interactions with BPA. In fact, Tyr326 might be in an ideal position to accept BPA in the ERRγ-LBP complex. When superimposition between ERRγ-LBD from the BPA/ERRγ-LBD complex and the ERRγ-LBD apo form (PDB code 1TFC) (*23*, *24*) was carefully checked, significant deviation was found for the Tyr326-phenol group (Fig. 5A and B). As shown in Fig. 5B, the Tyr326-phenol group in the BPA/ERRγ-LBD complex is pulled towards Asn346, shifting it through an angle of approximately 10°. This deviation keeps Tyr326-phenol group in the range of still stronger hydrogen bonds with Asn346, at a distance of 2.7 Å. All other amino acid residues in LBD are in exact agreement. In particular, the inside of the pocket is totally compatible with that of the apo form (Fig. 5A).

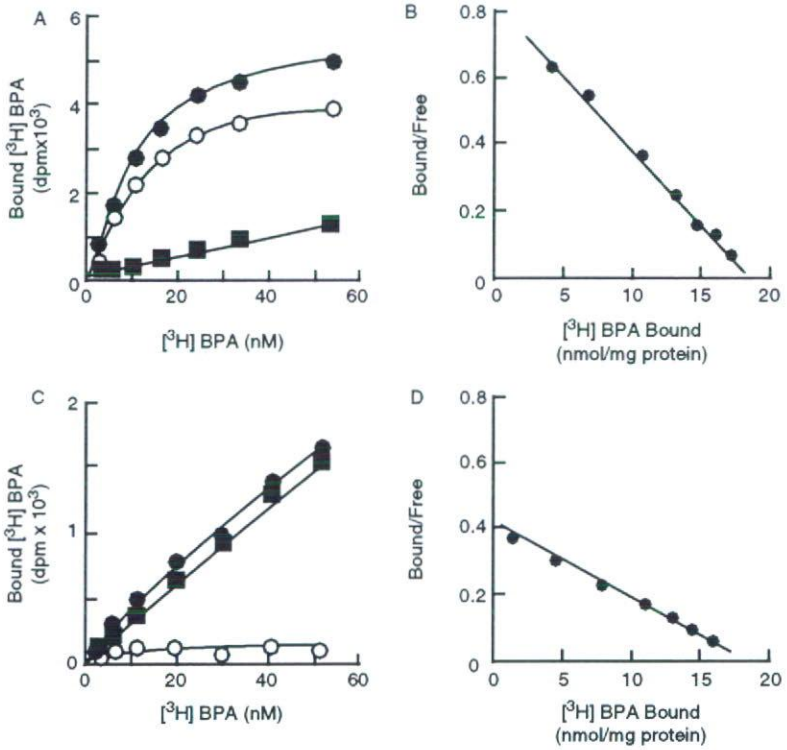

Fig. 6. **Receptor binding assays using tritium-labelled BPA.** (A) A sufficient specific binding of [^{3}H]BPA obtained in the saturation binding assay for wild-type ERRγ-LBD receptor. Closed circle, total binding; closed square, non-specific binding; and open circle, specific binding. (B) Scatchard plot analysis of [^{3}H]BPA for wild-type ERRγ-LBD. $K_D = 5.54 \pm 0.31$ nM, $B_{max} = 18.2 \pm 0.3$ nmol/mg protein. (C) No specific binding of [^{3}H]BPA shown in the saturation binding assay for ERRγ-LBD mutant receptor with E275A and R316A simultaneous substitutions. (D) Scatchard plot analysis of [^{3}H]BPA for ERRγ-LBD mutant receptor with N346A substitution. $K_D = 9.51 \pm 0.22$ nM, $B_{max} = 18.5 \pm 0.3$ nmol/mg protein. The Asn→Ala replacement was found to reduce approximately twice the dissociation constant, indicating that the Asn residue is important to the receptor binding of BPA presumably by the hydrogen-bonding between ERRγ-Asn-βCONH$_2$ and the BPA's phenol-hydroxyl group.

Interaction of Methyl Groups in Bisphenol A—BPA also has two methyl groups on the sp^3-C atom. One of these faces Phe435 (H11), and indeed the BPA-CH_3 and Phe435-phenyl groups are in close proximity (3.7 Å) to each other (Fig. 4F). On the other hand, another BPA-CH_3 group faces the Met306 sulphur atom with a non-covalent electron pair (3.6 Å between BPA-$\underline{C}H_3$ and Met306-$\underline{S}$) (Fig. 4F) making a form of electrostatic interaction. These interactions have been demonstrated by the drastically decreased binding activity that occurs in hexafluoro-BPA (designated as bisphenol AF), HO–C_6H_4–$C(CF_3)_2$–C_6H_4–OH, in which both CH_3 groups in BPA are replaced with trifluoromethyl CF_3 group. Electron-rich CF_3 would repel the electron-rich Phe-phenyl group and the Met-sulphur atom.

As mentioned earlier, BPA in the ERRγ-LBD complex is superimposed almost completely with BPA in the minimum-energy conformation (Fig. 4B). This implies that BPA fits spontaneously to the binding pocket of ERRγ-LBD without any conformational constraints, and binds specifically to each attachment position. It is likely that ERRγ possesses a binding pocket specifically adapted to the space requirements of the naturally occurring BPA-like ligand.

Superimposition of Bisphenol A/ERRγ-LBD Complex with Other Complexes—Superimposition of BPA and DES (1S9P) (*23*) in the ERRγ-LBD complexes shows conformational differences that can readily account for the differences in binding modes to the binding pocket. The phenol A ring of BPA superimposes almost completely with the corresponding A ring of DES, whereas the B rings orient in completely different directions (Fig. 5C). As a result, the phenol B ring of BPA heads towards H7 to capture Asn346 by its hydrogen bond, while that of DES goes towards H11 to restrain His434 also by a hydrogen bond.

Superimposition of the BPA complex and the 4-OHT complex (1S9Q) (*23*) of ERRγ-LBD, on the other hand, shows structural differences that make clear the difference in their activity mediated through the ERRγ. As before, the phenol A ring of BPA superimposes almost completely with the corresponding A ring of 4-OHT (Fig. 5D). Incontrast, the aromatic B ring of 4-OHT goes towards H11 with no hydrogen bond. The aromatic C ring of 4-OHT directs itself towards H12.

Greschik *et al.* (*23*) have reported that the binding of DES and 4-OHT to ERRγ-LBD dissociates the H12 region from the LBD body. DES- and 4-OHT-mediated

activities were explained by the three-dimensional structure of the DES/or 4-OHT/ERRγ-LBD complex, in which helix 12 is widely separated from a position in the activation conformation. Indeed, their H12s are out of superimpositions between the BPA/ERRγ-LBD and the DES/ or 4–OHT/ERRγ-LBD complexes (Fig. 5C and D). This repositioning of H12 by DES and 4-OHT deactivates ERRγ, because the receptor becomes unable to recruit coactivator proteins at the appropriate position. The LBD structure of ERRγ apo form has also been solved (*23, 24*), and as expected from its very high constitutive activity, H12 of this non-liganded ERRγ-LBD is folded in the activation conformation (Fig. 5A).

Bisphenol A Holds ERRγ-LBD in the Activation Conformation—One of the most important findings in the present study is that H12 in the BPA/ERRγ-LBD complex is in the transcriptionally active conformation. H12 is associated firmly with the LBD body, where the coactivator binds. When we compared this crystal structure with the reported crystal structure (1TFC) of the apo form of ERRγ-LBD (*23*), almost no conformational changes were shown for almost all the atoms including both the main and side chains from H1 to H12 (Fig. 5A). Superimposition of the ERRγ-LBD from the BPA/ERRγ-LBD complex and the apo ERRγ-LBD shows their exact and entire agreement. In particular, the positioning and conformation of H12 is totally compatible with that of the apo form (Fig. 5A and B). Although H12's activation conformation in the apo form appeared to be maintained by the presence of a peptide derived from the coactivator protein SRC-1, H12 in the BPA/ERRγ-LBD complex is in fact in the activation conformation without the SRC-1 peptide.

These conformational consequences verify the high functional activity of BPA. ERRγ *per se* elicits a very high basal activity in the luciferase reporter gene assay. BPA was found to maintain this high spontaneous constitutive activity in ERRγ for a range of concentrations from 10^{-10} to 10^{-5} M BPA (*10*). Furthermore, BPA reverses the deactivation activity of 4-OHT, indicating that BPA displaces 4-OHT and repositions the H12 from the transcriptionally inactive conformation to the active conformation. It should be noted that the compounds that deactivate the receptor are termed as 'inverse agonist,' whereas those that inhibit such inverse agonists are defined as 'inverse antagonist.' Thus, BPA indeed acts as an inverse antagonist against the inverse agonist 4-OHT in ERRγ.

Structural Demonstration of the Binding Sites by Site-directed Mutagenesis—The amino acid residues in the BPA-binding site of ERRγ-LBD were substituted with Ala by means of the site-directed mutagenesis. Those included Glu275, Met306, Leu309, Arg316, Tyr326, Asn346 and Phe435 in the binding pocket. The resulting mutant receptors were examined by the saturation binding assay using tritium-labelled BPA (Fig. 6A and B). When Glu275 and Arg316 were substituted simultaneously, the mutant receptor exhibited almost no specific binding (Fig. 6C), indicating that these residues are critically important to bind BPA to the pocket. In contrast, [^{3}H]BPA was found to bind to Asn346Ala mutant receptor (B_{max} = 18.5 nmol/mg) as well as wild-type receptor (18.2 nmol/mg), although its binding affinity for the mutant was approximately 2-fold weaker (K_D = 9.51 nM) than that for the wild-type (5.54 nM) (Fig. 6D). All other mutant receptors exhibited considerably reduced specific binding and drastically weakened binding ability (10–20-fold larger K_D values). The results clearly evidenced that the structural elements complementary to BPA are indeed its binding sites.

Conclusion and Perspectives—The present study clearly indicates that the nuclear receptor ERRγ possesses a space in its LBD to which BPA can bind highly specifically and selectively. It is still not clear whether, under physiological conditions, ERRγ can function without an endogenous ligand, nor what ERRγ's physiological functions may be. The results we present imply that ERRγ may in fact have a BPA-like endogenous ligand, and will facilitate the design of novel specific agonist and antagonist compounds.

The binding affinity of [^{3}H]BPA to ERRγ-LBD is extremely high, with a K_D value of 5.5 nM. Thus, it is an immediate and important requirement to evaluate whether the previously reported effects of BPA at low doses are mediated through ERRγ and its specific target gene(s). At the same time, it is necessary to clarify what the physiological roles of ERRγ are, and to examine the extent of, and direction in which, BPA may influence these. This is particularly important because ERRγ is expressed in a tissue-restricted manner, for example, very strongly in the mammalian foetal brain and also in the placenta, at sites that could have important outcomes for the newborn.

We thank Prof. Ian A. Meinertzhagen, Dalhousie University, Canada, for reading the manuscript. This study was supported by Health and Labour Sciences Research Grants to Y.S., for Research on Risk of Chemical Substances, from the Ministry of Health, Labor and Welfare of Japan. This work was also supported in part by grants-in-aid from the Ministry of Education, Culture, Sports, Science and Technology of Japan to Y.S. We thank the staff of the SPring-8 BL38B1 beamline for help with the X-ray diffraction experiments. The work was supported by a grant for the National Project on Protein Structural and Functional Analyses from the Ministry of Education, Culture, Sports, Science and Technology of Japan. Atomic coordinates for the structure have been deposited in the Protein Data Bank with accession code 2E2R.

REFERENCES

1. Krishnan, A.V., Stathis, P., Permuth, S.F., Tokes, L., and Feldman, D. (1993) Bisphenol-A: an estrogenic substance is released from polycarbonate flasks during autoclaving. *Endocrinology* **132**, 2279–2286
2. Olea, N., Pulgar, R., Pérez, P., Olea-Serrano, F., Rivas, A., Novillo-Fertrell, A., Pedraza, V., Soto, A.M., and Sonnenschein, C. (1996) Estrogenicity of resin-based composites and sealants used in dentistry. *Environ. Health Perspect.* **104**, 298–305
3. Nagel, S.C., vom Saal, F.S., Thayer, K.A., Dhar, M.G., Boechler, M., and Welshons, W.V. (1997) Relative binding affinity-serum modified access (RBA-SMA) assay predicts the relative *in vivo* bioactivity of the xenoestrogens

bisphenol A and octylphenol. *Environ. Health Perspect.* **105**, 70–76
4. Markey, C.M., Luque, E.H., de Toro, M.M., Sonnenschein, C., and Soto, A.M. (2001) In utero exposure to bisphenol A alters the development and tissue organization of the mouse mammary gland. *Biol. Reprod.* **65**, 1215–1223
5. Kubo, K., Arai, O., Omura, M., Watanabe, R., Ogata, R., and Aou, S. (2003) Low dose effects of bisphenol A on sexual differentiation of the brain and behavior in rats. *Neurosci. Res.* **45**, 345–356
6. Kawai, K., Nozaki, T., Nishikata, H., Aou, S., Takii, M., and Kubo, C. (2003) Aggressive behavior and serum testosterone concentration during the maturation process of male mice: the effects of fetal exposure to bisphenol A. *Environ. Health Perspect.* **111**, 175–178
7. vom Saal, F.S. and Hughes, C. (2005) An extensive new literature concerning low-dose effects of bisphenol A shows the need for a new risk assessment. *Environ. Health Perspect.* **113**, 926–933
8. Welshons, W.V., Thayer, K.A., Judy, B.M., Taylor, J.A., Curran, E.M., and vom Saal, F.S. (2003) Large effects from small exposures. I. Mechanisms for endocrine-disrupting chemicals with estrogenic activity. *Environ. Health Perspect.* **111**, 994–1006
9. National Toxicology Program (NTP). U.S. Department of Health and Human Services, National Institute of Environmental Health Sciences, National Institute of Health. National Toxicology Program's Report of Endocrine Disruptors Low-Dose Peer Review (2001). Available on the NTP web site: http://ntp-server.niehs.nih.gov/htdocs/liason/LowDoseWebPage.html.
10. Takayanagi, S., Tokunaga, T., Liu, X., Okada, H., Matsushima, A., and Shimohigashi, Y. (2006) Endocrine disruptor bisphenol A strongly binds to human estrogen-related receptor γ(ERRγ) with high constitutive activity. *Toxicol. lett.* **167**, 95–105
11. Eudy, J.D., Yao, S., Weston, M.D., Ma-Edmonds, M., Talmadge, C.B., Cheng, J.J., Kimberling, W.J., and Sumegi, J. (1998) Isolation of a gene encoding a novel member of the nuclear receptor superfamily from the critical region of Usher syndrome type IIa at 1q41. *Genomics* **50**, 382–384
12. Giguère, V. (2002) To ERR in the estrogen pathway. *Trends Endocrinol. Metab.* **13**, 220–225
13. Horard, B. and Vanacker, J.M. (2003) Estrogen receptor-related receptors: orphan receptors desperately seeking a ligand. *J. Mol. Endocrinol.* **31**, 349–357
14. Bradford, M.M. (1976) A rapid and sensitive method for the quantitation of microgram quantities of protein utilizing the principle of protein-dye binding. *Anal. Biochem.* **72**, 248–254
15. Nakai, M., Tabira, Y., Asai, D., Yakabe, Y., Shimyozu, T., Noguchi, M., Takatsuki, M., and Shimohigashi, Y. (1999) Binding characteristics of dialkyl phthalates for the estrogen receptor. *Biochem. Biophys. Res. Commun.* **254**, 311–314
16. Otwinowski, Z. and Minor, W. (1997) Processing of X-ray diffraction data collected in oscillation mode. *Method Enzymol.* **276**, 307–326
17. Vagin, A. and Teplyakov, A. (1997) MOLREP: an automated program for molecular replacement. *J. Appl. Cryst.* **30**, 1022–1025
18. Collaborative Computational Project (1994) The CCP4 Suite: programs for protein crystallography. *Acta Cryltallogr. Sect. D Biol. Crystallogr.* **50**, 760–763
19. Murshudov, G.N., Vagin, A.A., and Dodson, E.J. (1997) Refinement of macromolecular structures by the maximum-likelihood method. *Acta Crystallogr. D Biol. Crystallogr.* **53**, 240–255
20. Emsley, P. and Cowtan, K. (2004) Coot: model-building tools for molecular graphics. *Acta Crystallogr. D Biol. Crystallogr.* **60**, 2126–2132
21. Laskowski, R.A., McArthur, M.W., Moss, D.S., and Thornton, J.M. (1993) A program to check the stereochemical quality of protein structures. *J. Appl. Cryst.* **26**, 283–291
22. Huppunen, J. and Aarnisalo, P. (2004) Dimerization modulates the activity of the orphan nuclear receptor ERR γ. *Biochem. Biophys. Res. Commun.* **314**, 964–970
23. Greschik, H., Flaig, R., Renaud, J.P., and Moras, D. (2004) Structural basis for the deactivation of the estrogen-related receptor γ by diethylstilbestrol or 4-hydroxytamoxifen and determinants of selectivity. *J. Biol. Chem.* **279**, 33639–33646
24. Greschik, H., Wurtz, J.M., Sanglier, S., Bourguet, W., van Dorsselaer, A., Moras, D., and Renaud, J.P. (2002) Structural and functional evidence for ligand-independent transcriptional activation by the estrogen-related receptor 3. *Mol. Cell* **9**, 303–313
25. Nishio, M., Umezawa, Y., Hirota, M., and Takeuchi, Y. (1995) The CH/π interaction: Significance in molecular recognition. *Tetrahedron* **51**, 8665–8701
26. Umezawa, Y. and Nishio, M. (2005) CH/π hydrogen bonds as evidenced in the substrate specificity of acetylcholine esterase. *Biopolymers* **79**, 248–258
27. Ôki, M. and Iwamura, H. (1967) Steric effects on the O – H ···· π interaction in 2-hydroxybiphenyl. *J. Am. Chem. Soc.* **89**, 576–579
28. Subramanian, S. and Zaworotko, M.J. (1994) Exploitation of the hydrogen bond: Recent developments in the context of crystal engineering. *Coordin. Chem. Rev.* **137**, 357–401

Direct Evidence Revealing Structural Elements Essential for the High Binding Ability of Bisphenol A to Human Estrogen-Related Receptor-γ

Hiroyuki Okada, Takatoshi Tokunaga, Xiaohui Liu, Sayaka Takayanagi, Ayami Matsushima, and Yasuyuki Shimohigashi

Laboratory of Structure-Function Biochemistry, Department of Chemistry, The Research-Education Centre of Risk Science, Faculty and Graduate School of Sciences, Kyushu University, Fukuoka, Japan

Background: Various lines of evidence have shown that bisphenol A [BPA; HO-C_6H_4-$C(CH_3)_2$-C_6H_4-OH] acts as an endocrine disruptor when present in very low doses. We have recently demonstrated that BPA binds strongly to human estrogen-related receptor-γ (ERR-γ) in a binding assay using [^{3}H]4-hydroxytamoxifen ([^{3}H]4-OHT). We also demonstrated that BPA inhibits the deactivation activity of 4-OHT.

Objectives: In the present study, we intended to obtain direct evidence that BPA interacts with ERR-γ as a strong binder, and also to clarify the structural requirements of BPA for its binding to ERR-γ.

Methods: We examined [^{3}H]BPA in the saturation binding assay using the ligand binding domain of ERR-γ and analyzed the result using Scatchard plot analysis. A number of BPA derivatives were tested in the competitive binding assay using [^{3}H]BPA as a tracer and in the luciferase reporter gene assay.

Results: [^{3}H]BPA showed a K_D of 5.50 nM at a B_{max} of 14.4 nmol/mg. When we examined BPA derivatives to evaluate the structural essentials required for the binding of BPA to ERR-γ, we found that only one of the two phenol-hydroxyl groups was essential for the full binding. The maximal activity was attained when one of the methyl groups was removed. All of the potent BPA derivatives retained a high constitutive basal activity of ERR-γ in the luciferase reporter gene assay and exhibited a distinct inhibitory activity against 4-OHT.

Conclusion: These results indicate that the phenol derivatives are potent candidates for the endocrine disruptor that binds to ERR-γ.

Key words: bisphenol A, constitutive activity, endocrine disruptor, estrogen receptor, estrogen-related receptor-γ, inverse agonist, nuclear receptor. *Environ Health Perspect* 116:32–38 (2008). doi:10.1289/ehp.10587 available via *http://dx.doi.org/* [Online 5 October 2007]

Bisphenol A [BPA; 2,2-bis(4-hydroxyphenyl)propane] has a symmetrical chemical structure of HO-C_6H_4-$C(CH_3)_2$-C_6H_4-OH. BPA is used mainly in the production of polycarbonate plastics and epoxy resins. Its worldwide manufacture is approximately 3.2 million metric tons/year. BPA has been acknowledged to be an estrogenic chemical able to interact with human estrogen receptors (ER) (Dodds and Lawson 1938; Krishnan et al. 1993; Olea et al. 1996), and many lines of evidence have revealed that BPA, at even low doses, acts as an endocrine disruptor (Gupta 2000; Nagel et al. 1997; vom Saal et al. 1998; Welshons et al. 2003). However, its binding to and hormonal interaction with ER are extremely weak, 2–3 orders of magnitude lower than those of natural hormones, and thus the intrinsic significance of these low-dose effects is rather intangible and obscure (Safe et al. 2002). These facts led us to hypothesize that BPA may interact with nuclear receptors (NRs) other than ER.

We have recently demonstrated that BPA binds strongly to estrogen-related receptor-γ (ERR-γ) with high constitutive activity (Takayanagi et al. 2006). ERR-γ is a member of the human NR family and the estrogen-related receptor (ERR) subfamily of orphan NRs, which are closely related to the ERs ER-α and ER-β (Giguère 2002; Horard and Vanacker 2003). The ERR family includes three members—ERR-α, ERR-β, and ERR-γ—with ERR-γ being the most recently identified (Eudy et al. 1998; Hong et al. 1999). The amino acid sequences are quite highly conserved among ERRs and ERs, but 17β-estradiol (E_2), a natural ligand of ERs, does not bind to any of the ERR family members. Our discovery that BPA binds strongly to ERR-γ, but not to ERs, indicates that the effects of the so-called endocrine disruptors should be examined for all NRs without delay.

ERR-γ is expressed in a tissue-restricted manner—for example, very strongly in the mammalian brain during development, and then in the brain, lung, and many other tissues during adulthood (Eudy et al. 1998; Heard et al. 2000; Lorke et al. 2000). Our preliminary results have shown that the highest expression is brought about in the placenta (Takeda Y, Sumiyoshi M, Liu X, Matsushima A, Shimohigashi M, Shimohigashi Y, unpublished data). Strong binding of BPA to ERR-γ would affect not only the physiologic functions but also the metabolism of this NR as a transcription-activating factor. Although the intrinsic physiologic functions of ERR-γ have not yet been clarified, it is crucial that a structure–function study be performed to clarify the structural requirements for the binding of BPA to ERR-γ.

In a previous study (Takayanagi et al. 2006), we used tritium (^{3}H)-labeled 4-hydroxytamoxifen (4-OHT) as a tracer in a receptor binding assay for ERR-γ. 4-OHT binds strongly to ERR-γ and deactivates it as an inverse agonist, decreasing the very high level of spontaneous constitutive activity (Coward et al. 2001). As a substitute for [^{3}H]4-OHT, BPA was found to be as potent as 4-OHT in this binding assay. Furthermore, BPA was found to retain or rescue ERR-γ's high basal constitutive activity in the reporter gene assay for ERR-γ using HeLa cells. These results indicated that BPA and 4-OHT bind to ERR-γ with equal strength, but have structural differences that affect their occupation of ERR-γ's ligand binding pocket. In the complex formed between 4-OHT and the ERR-γ–ligand binding domain (LBD), 4-OHT remained at the ligand binding pocket of ERR-γ–LBD, but the α-helix 12 of the receptor was repositioned from the activation conformation (Greschik et al. 2004; Wang et al. 2006). In contrast, BPA was suggested to bind to the pocket without changing the positioning of helix 12, and thus preserved the high receptor constitutive activity of ERR-γ.

It is evident that the binding ability of BPA to ERR-γ should be examined by means of tritium-labeled BPA. Fortunately, [^{3}H]BPA is now commercially available; thus, in the present study we performed the first saturation binding assay for direct exploration of the binding characteristics of BPA. We then established a competitive receptor binding assay in which chemicals were assessed for their ability to displace [^{3}H]BPA from the receptor binding pocket. In particular, industrial chemical products of BPA analogs were inspected structurally in order to better understand the

Address correspondence to Y. Shimohigashi, Laboratory of Structure-Function Biochemistry, Department of Chemistry, The Research-Education Centre of Risk Science, Faculty of Sciences, Kyushu University, Fukuoka 812-8581, Japan. Telephone: 81-92-642-2584. Fax: 81-92-642-2584. E-mail: shimoscc@mbox.nc.kyushu-u.ac.jp

This study was supported by Health and Labour Sciences Research Grants for Research on the Risk of Chemical Substances from the Ministry of Health, Labor and Welfare of Japan.

The authors declare they have no competing financial interests.

Received 22 June 2007; accepted 4 October 2007.

structural elements of BPA that are required for binding to the ERR. Here we describe the structural elements of BPA that are required for the binding to ERR-γ–LBD and for maintaining the receptor in an active conformation.

Materials and Methods

Chemicals. We purchased 2,2-bis(4-hydroxyphenyl)propane and 4,4-isopropylidenediphenol, both denoted as BPA, from Tokyo Kasei Kogyo Co. (Tokyo, Japan), Nakarai Tesque (Kyoto, Japan), Aldrich (Madison, WI, USA), Junsei Chemical (Tokyo, Japan), Acros (Geel, Belgium), Lancaster Synthesis (Windham, NH, USA), Merck (Darmstadt, Germany), and Fluka (Buchs, Switzerland). The purity designated on the labels varied from 95 to 99%. We also obtained the following analogs of BPA: bisphenol AF [2,2-bis(4-hydroxyphenyl)hexafluoropropane; Tokyo Kasei], bisphenol AP [4,4′-(1-phenylethylidene)bisphenol; Tokyo Kasei], bisphenol B [2,2-bis(4-hydroxyphenyl)butane; Tokyo Kasei], bisphenol E [2,2-bis(4-hydroxyphenyl)ethane; Aldrich], and bisphenol F [bis(4-hydroxyphenyl)methane; Tokyo Kasei].

4-α-Cumylphenol [2-(4-hydroxyphenyl)-2-phenylpropane], 4-*tert*-amylphenol, 4-*tert*-butylphenol, 4-isopropylphenol, and 4-ethylphenol were obtained from Tokyo Kasei. 2,2-Diphenyl propane, and 4-*tert*-octylphenol were obtained from Aldrich, and *p*-cresol and phenol from Kishida Chemical (Osaka, Japan).

Preparation of receptor protein GST-fused ERR-γ–LBD. ERR-γ–LBD was amplified from a human kidney cDNA library (Clontech Laboratories, Mountain View, CA, USA) by polymerase chain reaction (PCR) using gene-specific primers and cloned into pGEX6P-1 (Amersham Biosciences, Piscataway, NJ, USA). Glutathione *S*-transferase (GST)–fused receptor protein expressed in *Escherichia coli* BL21α was purified on an affinity column of glutathione-sepharose 4B (GE Healthcare Bio-Sciences Co., Piscataway, NJ, USA) to obtain GST-ERR-γ–LBD. The glutathione used for elution of GST-ERR-γ–LBD from the column was removed by gel filtration on a column of Sephadex G-10 (15 × 100 mm; GE Healthcare Bio-Sciences Co.) equilibrated with 50 mM Tris-HCl (pH 8.0), and the protein content (506.24 μg/mL) was estimated by the Bradford method using a Protein Assay CBB Solution (Nakarai Tesque). Preparation of GST-fused ER-α–LBD was carried out as described previously (Takayanagi et al. 2006).

Radioligand binding assays for saturation binding. The saturation binding assay for GST-ERR-γ–LBD was conducted at 4°C using [^{3}H]BPA (5 Ci/mmol; Moravek Biochemicals, Brea, CA, USA) with or without BPA (10 μM in the final solution). Purified protein (0.32 μg/mL) was incubated with increasing concentrations of [^{3}H]BPA (2.1–24.3 nM) in a final volume of 100 μL of binding buffer [10 mM HEPES (pH 7.5), 50 mM sodium chloride, 2 mM magnesium chloride, 1 mM EDTA, 2 mM CHAPS {3-[(3-cholamidopropyl)dimethylammonio]-1-propanesulfonate}, and 2 mg/mL γ-globulin]. Nonspecific binding was determined in a parallel set of incubations that included 10 μM nonradiolabeled BPA. After incubation for 2 hr at 4°C, all the fractions were filtered by the direct vacuum filtration method (MultiScreen$_{HTS}$ HV, 0.45 μm pore size; Millipore, Billerica, MA, USA) for the B/F separation (the separation of receptor-bound ligand from free ligand) (Nakai et al. 1999). Filtration was carried out on a multiscreen separation system (Millipore). Before filtration, 100 μL of 1% dextran-coated charcoal (DCC) (Sigma) in phosphate buffer (pH 7.4) was added to the assay vessels, and the mixture was incubated for 10 min on ice. The radioactivity of the filtered solution was counted on a liquid scintillation counter (LS6500; Beckman Coulter, Fullerton, CA, USA). The saturation assay was performed in triplicate. The specific binding of [^{3}H]BPA was calculated by subtracting the nonspecific binding from the total binding.

Radioligand binding assays for competitive binding. BPA and the BPA-related chemicals were dissolved in a binding buffer containing 0.3–1.0% *N,N*-dimethylsulfoxide (DMSO). These compounds were examined for their ability to inhibit the binding of [^{3}H]BPA (3 nM in the final solution) to GST-ERR-γ–LBD (0.32 μg/mL in the final solution). The reaction mixtures were incubated for 2 hr at 4°C and free radioligand was removed with 1% DCC by filtration as described above. Radioactivity was determined on a liquid scintillation counter (TopCount NXT; PerkinElmer Life Sciences Tokyo, Japan). The IC_{50} values (the concentrations for the half-maximal inhibition) were calculated from the dose–response curves obtained using the nonlinear analysis program ALLFIT (De Lean et al. 1978). Each assay was performed in duplicate and repeated at least three times. The competitive binding assay for GST-ER-α–LBD was carried out as described above using [^{3}H]E_2 (5.74 TBq/mmol; Amersham Biosciences, Buckinghamshire, UK).

Cell culture and transient transfection assays. HeLa cells were maintained in Eagle's MEM (EMEM; Nissui, Tokyo, Japan) in the presence of 10% (vol/vol) fetal bovine serum at 37°C. For luciferase assays, HeLa cells were seeded at 5 × 10^5 cells/6-cm dish for 24 hr and then transfected with 4 μg of reporter gene (pGL3/3×ERRE) and 3 μg of ERR-γ expression plasmids (pcDNA3/ERR-γ) by Lipofectamine Plus reagent (Invitrogen Japan, Tokyo, Japan) according to the manufacturer's protocol. Approximately 24 hr after transfection, cells were harvested and plated into 96-well plates at 5 × 10^4 cells/well. The cells were then treated with varying doses of chemicals diluted with 1% bovine serum albumin/phosphate-buffered saline (BSA/PBS, vol/vol). To measure the antagonistic activity, a fixed concentration of compounds (10^{-5} M to 10^{-10} M in the final solution) was added along with 4-OHT. After 24 hr, luciferase activity was measured with the appropriate reagent using a Luciferase Assay System (Promega, Madison, WI, USA) according to the manufacturer's instructions. Light emission was measured using a Wallac 1420 ARVOsx multilabel counter (PerkinElmer). Cells treated with 1% BSA/PBS were used as a vehicle control. Each assay was performed in triplicate and repeated at least three times.

Results and Discussion

Highly specific binding of BPA to ERR-γ. To demonstrate the direct binding of BPA to ERR-γ, we first attempted to establish a saturation receptor binding assay using radiolabeled BPA. We analyzed the saturation binding of [^{3}H]BPA against the recombinant ERR-γ–LBD protein, to which GST was fused at the N-terminus. In the actual receptor binding assay, we used [^{3}H]BPA (2.0–24 nM) against purified protein at a concentration of 0.32 μg/mL, which corresponds to a concentration of 6.3 nM. The removal of receptor-free [^{3}H]BPA was carried out with 1% DCC. In this procedure, DCC mixtures were transferred to a 96-well HV-plate with a filter (0.45-μm pore size) for direct vacuum.

As shown in Figure 1A, the binding of BPA to ERR-γ was specific and saturated. Specific binding of [^{3}H]BPA to ERR-γ was estimated to be approximately 80%, which we judged to be a very high value. In other words, the level of nonspecific binding of [^{3}H]BPA was very low (Figure 1A). The high level of specific binding of [^{3}H]BPA clearly demonstrated that BPA has no structural elements for nonspecific binding to the receptor protein and exclusively occupies the binding pocket of ERR-γ–LBD. GST did not bind [^{3}H]BPA at all. It should be noted that the specific binding of [^{3}H]4-OHT was only about 50% (Takayanagi et al. 2006).

The Scatchard plot analysis showed a distinct single binding mode (Figure 1B). From the slope, the binding affinity constant (K_D) was calculated to be 5.50 nM. The receptor density (B_{max}) was estimated to be 14.4 nmol/mg protein, which is roughly compatible with the calculated value of 18.9 nmol/mg protein. The B_{max} value of [^{3}H]4-OHT is much smaller than that of [^{3}H]BPA. These results further demonstrate that ERR-γ binds [^{3}H]BPA very specifically and exclusively.

Binding ability of BPA to ERR-γ. We performed the competitive receptor binding assay using [^{3}H]BPA (3 nM in the final solution) for GST–ERR-γ–LBD (0.32 μg/mL in the final solution). To confirm that BPA is a truly specific ligand for ERR-γ, we tested all nonradiolabeled BPA compounds available in Japan, which we obtained from seven different reagent companies. Because the compounds all had different levels of purity (95–99%), we adjusted their initial concentration, 1.0×10^{-2} M, based on the purity indicated on the label.

We found that BPA displaces [^{3}H]BPA in a dose-dependent manner. Its binding curve was sigmoidal in a single binding mode (slope = ~ 1), which afforded an average IC_{50} value of 9.78 nM. We found all BPA compounds purchased to be equally potent. These results clearly demonstrate that BPA binds very strongly to the NR ERR-γ.

4-OHT as a potent displacer of BPA in ERR-γ. 4-OHT has been reported to potently displace [^{3}H]4-OHT in the binding to ERR-γ (Greschik et al. 2004; Takayanagi et al. 2006). In the present study, 4-OHT very potently displaced [^{3}H]BPA (IC_{50} = 10.9 nM) (Table 1). BPA and 4-OHT yielded sigmoidal binding curves indistinguishable from each other (data not shown), indicating that the two are almost equipotent. These results obtained using the [^{3}H]BPA tracer were almost identical to those obtained by [^{3}H]4-OHT (Takayanagi et al. 2006).

BPA and 4-OHT share only a phenol group, and thus the phenol groups of these compounds are highly likely to occupy the same binding site in the ERR-γ receptor. Because the phenol group of 4-OHT is anchored by hydrogen bonds to Glu275 and Arg316 of ERR-γ (Greschik et al. 2004), the phenol group of BPA may also bind to these ERR-γ residues. Indeed, this has been proven by our recent X-ray crystal structure analysis of the complex between BPA and human ERR-γ–LBD (Matsushima et al. 2007). Hereafter, we designate the benzene ring of this phenol group of BPA as the A-ring and the additional benzene ring as the B-ring.

BPA-methyl as a structural requirement for binding to ERR-γ. We evaluated the role of the two methyl (CH_3) groups on the sp^3-C atom of BPA in binding to ERR-γ by a series of analogs of BPA, HO-C_6H_4-$C(CH_3)_2$-C_6H_4-OH. First, we examined the effect of incorporation of the methyl group on the binding affinity of BPA. When CH_3 was

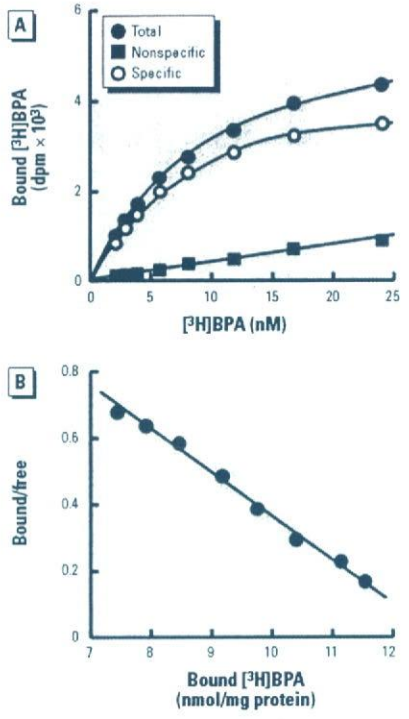

Figure 1. The saturation binding analysis of BPA for ERR-γ. (*A*) Saturation binding curve of [^{3}H]BPA for the recombinant human ERR-γ–LBD showing total, nonspecific, and specific binding. Determination of nonspecific binding was carried out by excess unlabeled BPA (10 μM). (*B*) Binding data analyzed by Scatchard plot analysis to estimate the dissociation constant (K_D) and the receptor density (B_{max}). The plot was linear, the K_D value was estimated to be 5.50 ± 0.87 nM, and B_{max} was 14.4 nmol/mg protein. The saturation binding analysis was performed in duplicate and repeated four times.

Table 1. Receptor binding affinity (mean ± SE) of BPA and its analogs, and 4-OHT for ERR-γ.

Chemical	Binding affinity (IC_{50}, nM)
BPA	9.78 ± 0.87
Bisphenol AF	358 ± 30.5
Bisphenol AP	123 ± 15.1
Bisphenol B	26.3 ± 2.65
Bisphenol E	8.14 ± 0.83
Bisphenol F	131 ± 17.9
4-OHT	10.9 ± 0.91

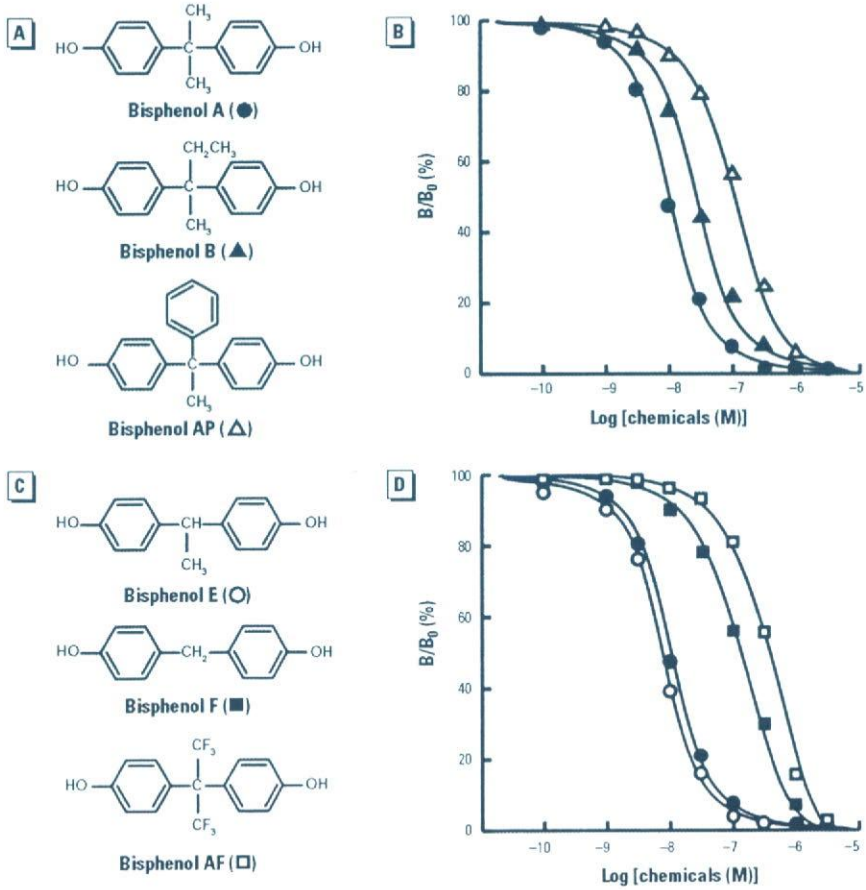

Figure 2. Chemical structure of BPA and its derivatives and their dose–response curves in the radioligand receptor binding assay for ERR-γ. (*A*) Chemical structures of BPA (two methyl groups) and its derivatives: bisphenol B (a methyl group and an ethyl group) and bisphenol AP (a methyl group and a phenyl group). (*B*) Binding activities of BPA, bisphenol B, and bisphenol AP examined by the competitive binding assay using [^{3}H]BPA and GST–ERR-γ–LBD. (*C*) Chemical structures of bisphenol E (one methyl group) and its derivatives, bisphenol F and bisphenol AF [two trifluoromethyl groups (CF_3)]. (*D*) Binding activities of BPA, bisphenol E, bisphenol F, and bisphenol AP examined by the competitive binding assay. (*B*) and (*D*) each show representative curves with the IC_{50} values closest to the mean IC_{50} from at least five independent assays for each compound. B/B_0 is the relative inhibitory activity estimated from the calculation of the percentage of displacement by the chemical tested (B) against the specific binding (B_0 = 100%) of [^{3}H]BPA.

incorporated into the parent methyl group to produce HO-C_6H_4-$C(CH_3)(CH_2CH_3)$-C_6H_4-OH (Figure 2A), we found the resulting bisphenol B to be approximately half as potent (IC_{50} = 26.3 nM) as BPA (Table 1). This result clearly indicates that a bulky group on the central sp^3-C atom is obviously disadvantageous in terms of the binding of BPA to ERR-γ's binding pocket.

On the other hand, an enhancement of activity was observed when one of the methyl groups was eliminated from BPA. The resulting bisphenol E [HO-C_6H_4-$CH(CH_3)$-C_6H_4-OH] (Figure 2C) exhibited slightly better binding activity (IC_{50} = 8.14 nM) than BPA (Table 1). Bisphenol E is indeed the most potent chemical to date for the NR ERR-γ (Figure 2D). The maximal activity was attained when one of the methyl groups was removed from BPA. Apparently, the concomitance of two methyl groups on the central sp^3-C atom of BPA is disadvantageous and unfavorable.

The fact that a single methyl group had the best fit for ERR-γ was further demonstrated by the diminished activity of bisphenol AP, which has a phenyl group in place of the hydrogen atom that is found in bisphenol E (Figure 2A). Bisphenol AP exhibited approximately 15-fold weaker binding affinity for ERR-γ than bisphenol E, with IC_{50} = 123 nM (Figure 2B, Table 1). Steric hindrance by the benzene ring, as well as its electron-rich characteristics, might be responsible for this drop in the receptor binding affinity of bisphenol AP.

The importance of the remaining methyl group in bisphenol E became evident from the drastically reduced activity of bisphenol F [HO-C_6H_4-CH_2-C_6H_4-OH]. This compound was approximately 16-fold less potent than bisphenol E, exhibiting an IC_{50} value of 131 nM (Table 1). All of these results clearly indicate that one of the two methyl groups is involved in the intermolecular interaction with the receptor residue(s). The interaction involving the CH_3 group is a kind of hydrophobic interaction, such as CH_3-alkyl and CH/π interactions.

The fundamental nature of this interaction involving the CH_3 group became rather apparent from the binding result of bisphenol AF [HO-C_6H_4-$C(CF_3)_2$-C_6H_4-OH]. The $CH_3 \rightarrow CF_3$ substitution in BPA creates this compound (Figure 2C), which has two electron-rich trifluoromethyl CF_3 groups instead of the rather electron-poor methyl CH_3 group. The molecular size of CF_3 is almost equal to that of CH_3. A drastically reduced activity of bisphenol AF, about 35-fold less potent (358 nM) than BPA (Table 1), thus demonstrates that the BPA's CH_3 group is in an electrostatic interaction with the electron-rich residue(s) of the receptor. Replacement of CH_3 with CF_3 is definitely disadvantageous, because CF_3 is very electron-rich and thus brings about a strong repulsion with such electron-rich residues of the receptor. One of the electron-rich candidates of the receptor is the aromatic ring of Phe, Tyr, His, and Trp. Based on the reported X-ray crystal structure of ERR-γ, feasible candidates are Phe-435 and Phe-450 (Greschik et al. 2002, 2004; Matsushima et al. 2007; Wang et al. 2006).

A single phenol-hydroxyl group is enough for BPA to bind to ERR-γ. BPA has a very simple symmetrical chemical structure of HO-C_6H_4-$C(CH_3)_2$-C_6H_4-OH (Figure 2A). When one of the phenol-hydroxyl groups (–OH) of BPA was eliminated, the resulting 4-α-cumylphenol (HO-C_6H_4-$C(CH_3)_2$-C_6H_5; Figure 3A) still bound very strongly to ERR-γ. 4-α-Cumylphenol was as potent as BPA (Figure 3B), having an IC_{50} value of 10.6 nM (Table 2). Contrary to the expectation that both of the phenol-hydroxyl groups of BPA would participate in the hydrogen bonds, this result indicates that the second hydroxyl group does not necessarily participate in the hydrogen bonding. Given that this hydroxyl group forms a hydrogen bond with the ERR-γ receptor residue, the bond would be considered extremely weak, as suggested by the X-ray crystal analysis of 4-α-cumylphenol–ERR-γ complex (Matsushima A, Teramoto T, Okada H, Liu X, Tokunaga T, Kakuta Y, Shimohigashi Y, unpublished data).

When both of the phenol-hydroxyl groups were eliminated from BPA, the resulting 2,2-diphenyl propane [C_6H_5-$C(CH_3)_2$-C_6H_5] was almost completely inactive (Figure 3B, Table 2). This compound elicits only about 30% inhibition of the binding of [^{3}H]BPA at the 1-μM concentration, whereas BPA almost completely inhibits the binding of [^{3}H]BPA at this concentration (Figure 3B). It is clear that one of the phenol-hydroxyl groups of BPA is indispensable for the interaction with a binding pocket of ERR-γ. These results, together with the fact that 4-α-cumylphenol and BPA are equipotent, emphasizes the significance of one of the two phenol groups in the interaction of BPA with ERR-γ. As described above, this hydroxyl group should be attached to the benzene A-ring. It became apparent that the phenol-hydroxyl group attached to another phenol-benzene ring (B-ring) is not necessarily required for binding of BPA to ERR-γ.

BPA-phenol as a structural requirement for binding to ERR-γ. As described above, 4-α-cumylphenol is as active as BPA. The importance of the benzene B-ring can be examined by replacing the B-ring with the alkyl groups. When the benzene B-ring of 4-α-cumylphenol was substituted with either methyl or ethyl, the resulting 4-*tert*-butylphenol [HO-C_6H_4-$C(CH_3)_2$-CH_3] and

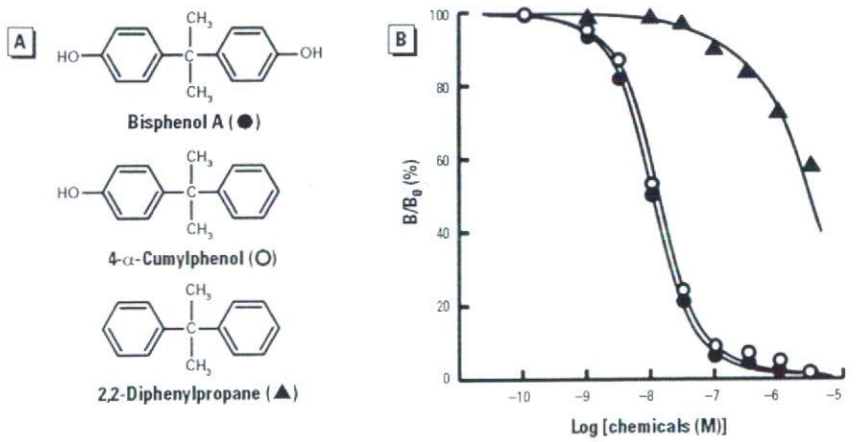

Figure 3. Chemical structure of BPA and its derivatives lacking the hydroxyl group(s) and their dose–response curves in the radioligand receptor binding assay for ERR-γ. (*A*) Chemical structure of BPA and its derivatives lacking the hydroxyl group(s): 4-α-cumylphenol (without one hydroxyl group from BPA), and 2,2-diphenylpropane (without either hydroxyl groups from BPA). (*B*) Binding activities of BPA, 4-α-cumylphenol, and 2,2-diphenylpropane examined by the competitive binding assay using [^{3}H]BPA and GST-ERR-γ–LBD; representative curves indicate the IC_{50} value closest to the mean IC_{50} from at least five independent assays for each compound.

Table 2. The receptor binding affinity (mean ± SE) of BPA and its derivatives lacking of the phenol group for human ERR-γ.

Chemical	Binding affinity (IC_{50}, nM)
BPA	9.78 ± 0.87
4-α-Cumylphenol	10.6 ± 0.87
2,2-Diphenylpropane	ND
4-*tert*-Butylphenol	26.1 ± 2.45
4-*tert*-Amylphenol	33.2 ± 2.85
4-Isopropylphenol	71.1 ± 7.73
4-*tert*-Octylphenol	238 ± 28.1
4-Ethylphenol	289 ± 45.9
p-Cresol	1,290 ± 72.5
Phenol	ND

ND, not determined (IC_{50} value could not be calculated because of extremely weak binding activity, even at a 10 μM concentration).

4-*tert*-amylphenol [HO-C_6H_4-$C(CH_3)_2$-CH_2CH_3] (Figure 4A) were considerably potent (Figure 4B), with values of 26.1 nM and 33.2 nM, respectively (Table 2). This reveals that alkyl groups can be substituted for the aromatic benzene ring without affecting the basal binding capability.

However, because both 4-*tert*-butylphenol and 4-*tert*-amylphenol are still a few times less active than 4-α-cumylphenol, a specific binding site of ERR-γ appears to prefer the aromatic benzene ring to the alkyl groups. This suggests that BPA's second phenol-phenyl group (benzene B-ring) is in the π interaction with the receptor residue(s), that is, either a XH/π interaction (X = N, O, and C) or a π/π interaction. The most plausible candidate for the receptor residue in this interaction is the Tyr residue at position 326 of ERR-γ. Indeed, the phenol-hydroxyl group of this Tyr-326 was found in the OH/π interaction with the B-ring of BPA (Matsushima et al. 2007).

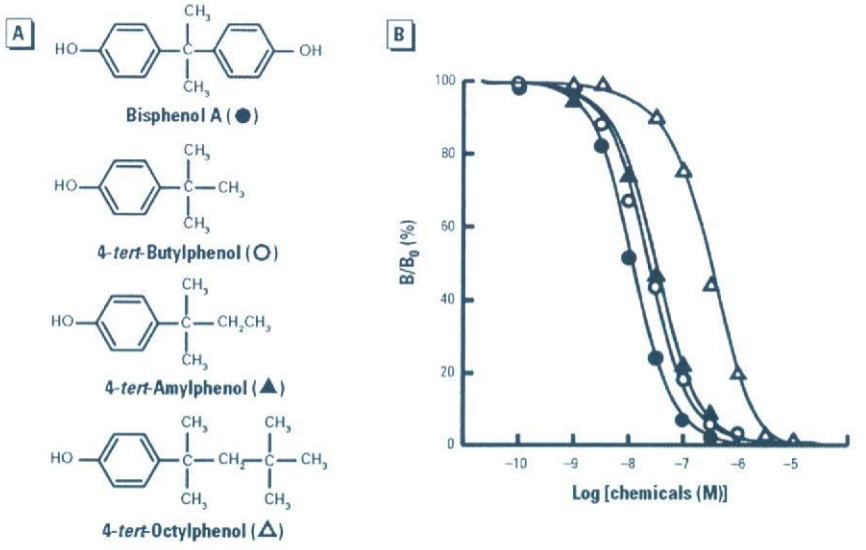

Figure 4. Chemical structure of BPA and its derivatives lacking the phenol group and their dose–response curves in the radioligand receptor binding assay for ERR-γ. (*A*) Chemical structure of BPA and its derivatives with the alkyl group at the position of phenol group: 4-*tert*-butylphenol (a methyl group); 4-*tert*-amylphenol (an ethyl group); and 4-*tert*-octylphenol (a *tert*-butyl methyl group). (*B*) Binding activities of BPA, 4-*tert*-butylphenol, 4-*tert*-amylphenol, and 4-*tert*-octylphenol examined by the competitive binding assay using [^{3}H]BPA and GST-ERR-γ–LBD; representative curves indicate the IC_{50} value closest to the mean IC_{50} from at least five independent assays for each compound.

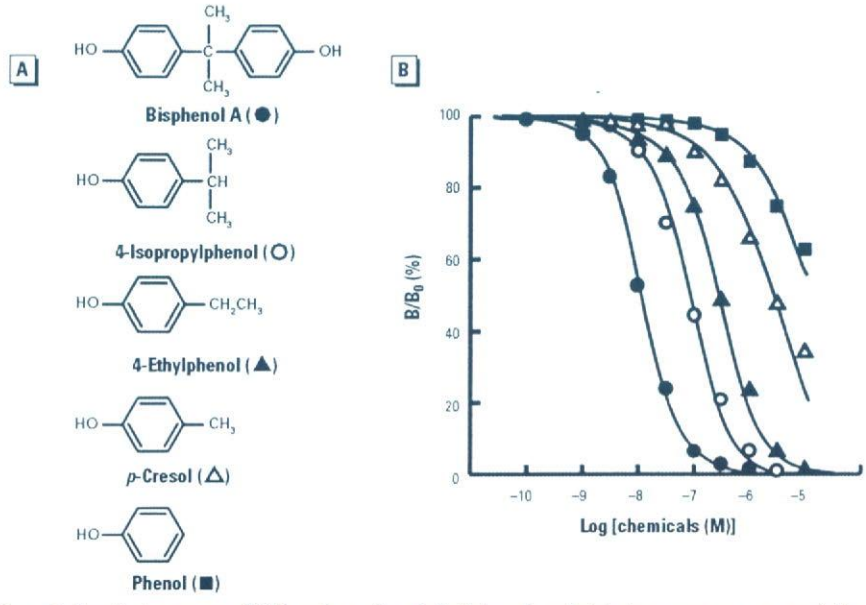

Figure 5. Chemical structure of BPA and a series of alkyl phenols and their dose–response curves in the radioligand receptor binding assay for ERR-γ. (*A*) Chemical structure of BPA and its derivatives with the alkyl group at the *para* position: 4-isopropylphenol (a 4-isopropyl group); 4-ethylphenol (an ethyl group); *p*-cresol (a methyl group); and phenol (a hydrogen atom). (*B*) Binding activities of BPA, 4-isopropylphenol, 4-ethylphenol, *p*-cresol, and phenol examined by the competitive binding assay using [^{3}H]BPA and GST-ERR-γ–LBD; representative curves indicate the IC_{50} value closest to the mean IC_{50} from at least five independent assays for each compound.

In a BPA molecule, two C_6H_4-OH (phenol) groups are connected to the sp^3 carbon atom (sp^3-C) together with two CH_3 (methyl) groups. The most simple structure–activity study is to compare the activity of compounds lacking one of these groups. The compound that lacks the phenol group is 4-isopropylphenol [HO-C_6H_4-$CH(CH_3)_2$] (Figure 5A), and this *para*-isopropyl phenol was fairly potent at displacing [^{3}H]BPA (Figure 5B), with an IC_{50} value of 71.1 nM (Table 2). However, 4-isopropylphenol was still approximately 7-fold less active than BPA, indicating that the phenol backbone structure is an essential structural element for the binding to ERR-γ.

When one of the two methyl groups was eliminated from 4-isopropylphenol, the resulting 4-ethylphenol [HO-C_6H_4-CH_2-CH_3] (Figure 5A) was found to be very weakly active (289 nM) (Table 2). Elimination of another methyl group still afforded a compound of inactive *p*-cresol [HO-C_6H_4-CH_3], but with the IC_{50} value being approximately 1.3 μM. Phenol [HO-C_6H_5] tended to bind to ERR-γ (Figure 5B). These results clearly indicate that the phenol group is a core structure for the attachment of BPA to ERR-γ.

4-Alkyl phenols as putative potent binders to ERR-γ. Attachment of the methyl group to 4-isopropylphenol [HO-C_6H_4-$CH(CH_3)_2$] to create 4-*tert*-butylphenol [HO-C_6H_4-$C(CH_3)_3$] considerably facilitates the binding of the phenol derivative to ERR-γ (Table 2). 4-*tert*-Amylphenol [HO-C_6H_4-$C(CH_3)_2$-CH_2CH_3] is almost as active as 4-*tert*-butylphenol. However, 4-*tert*-octylphenol [HO-C_6H_4-$C(CH_3)_2$-CH_2-$C(CH_3)_3$] (Figure 4B) was significantly weaker (approximately 10 times less potent) than 4-*tert*-butylphenol (Table 2). Thus, the activities of HO-C_6H_4-$C(CH_3)_2$-$CH(CH_3)_2$, HO-C_6H_4-$C(CH_3)_2$-$CH(CH_3)_3$, HO-C_6H_4-$C(CH_3)_2$-CH_2-CH_2-CH_3, and HO-C_6H_4-$C(CH_3)_2$-CH_2-$CH(CH_3)_2$ are expected to be intermediate between those of 4-*tert*-amylphenol and 4-*tert*-octylphenol, although these molecules are not commercially available. It appears that, among the 4-alkylphenols of HO-C_6H_4-$C(CH_3)_2$-C_nH_{2n+1} (=R), 4-*tert*-butylphenol (R = CH_3) and 4-*tert*-amylphenol (R = CH_2-CH_3) show the maximum competitive activity with the binding of ERR-γ.

The structural comparison of HO-C_6H_4-$C(CH_3)_2$-CH_3 (4-*tert*-butylphenol), HO-C_6H_4-$C(CH_3)_2$-CH_2CH_3 (4-*tert*-amylphenol),

and BPA HO-C_6H_4-$C(CH_3)_2$-C_6H_4-OH clearly indicated that the R group should not be bulky for high receptor binding activity. A plain π electron-rich benzene aromatic ring is thus optimal for interaction with the receptor residue of ERR-γ-Tyr326.

Inhibitory activity of BPA derivatives for ERR-γ. We found that BPA retained a high constitutive basal activity of ERR-γ in the luciferase reporter gene assay (Figure 6A). ERR-γ is in a full activation with no ligand; it is one of the self-activated NRs and is deactivated by the so-called "inverse agonists" such as 4-OHT (Greschik et al. 2004; Takayanagi et al. 2006). Although BPA shows no apparent effect on the high basal activity of ERR-γ, BPA evidently antagonizes or inhibits the deactivation activity of 4-OHT in a dose-dependent manner (Figure 6B), as reported by Takayanagi et al. (2006). This neutral antagonist is a distinct inhibitor or suppressor of the inverse agonist, reversing the deactivation conformation to the activation conformation.

All of the potent BPA derivatives (i.e., bisphenol E, bisphenol AF, 4-α-cumylphenol, and 4-*tert*-butylphenol) were found, just like BPA, to retain a high constitutive basal activity of ERR-γ in the same luciferase reporter gene assay (Figure 6C). In addition, these compounds inhibited the inverse agonist activity of 4-OHT and thus were specific inhibitors against the inverse agonist 4-OHT. Their abilities to antagonize 4-OHT are approximately one order lower than their binding potencies to ERR-γ (Figure 6B,D). This discrepancy is probably caused by the inclusion of a number of co-effecter proteins for eliciting a gene expression in the luciferase reporter gene assay.

Receptor selectivity of BPA derivatives for ERR-γ over ER-α. We classified BPA and its derivatives into the four groups, depending on their receptor binding affinity for ERR-γ: that is, group A, BPA and chemicals as potent as BPA; group B, chemicals considerably potent; group C, chemicals moderately potent; and group D, inactive chemicals. All chemicals were then examined for their ability to bind to ER-α, and the affinity measured was compared respectively with that for ERR-γ (Table 3). As reported previously (Takayanagi et al. 2006), BPA is highly selective for ERR-γ. It binds to ER-α only weakly; we calculated BPA's receptor selectivity to be 105, which suggests that BPA prefers ERR-γ 105 times more strongly than ER-α. Other group A compounds, namely, bisphenol E and 4-α-cumylphenol, were also greatly selective for ERR-γ (Table 3). In particular, bisphenol E was found to be exclusively selective and specific for ERR-γ because it was almost completely inactive for ER-α.

para-Alkyl phenols in group B ($IC_{50}^{ERR\text{-}\gamma}$ = of 26–71 nM) were also almost completely inactive for ER-α (Table 3). Those include

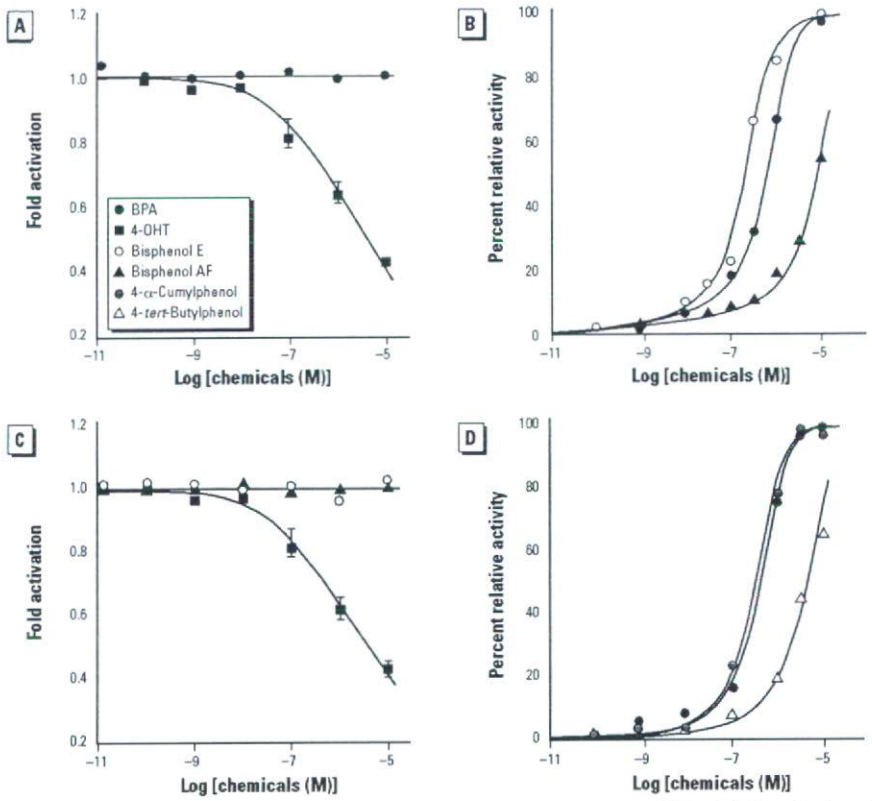

Figure 6. Luciferase-reporter gene assay of BPA and its derivatives for human ERR-γ. (*A*) Deactivation of the fully activated human ERR-γ by the inverse agonist 4-OHT and sustainment by BPA. (*B*) Reversing activity of BPA, bisphenol E, and bisphenol AF against the inverse agonist activity of 1.0 μM 4-OHT; 1.0 μM 4-OHT exhibited approximately 0.4-fold deactivation, and the inhibitory activities are shown by the percentage of relative activity. (*C*) Sustainment of the fully activated human ERR-γ by bisphenol E and bisphenol AF together with inverse agonist activity by 4-OHT. (*D*) Reversing activity of BPA, 4-α-cumylphenol, and 4-*tert*-butylphenol; the inverse agonist activity of 4-OHT was clearly reversed by all bisphenols tested in a dose-dependent manner. Data are from a single experiment performed in triplicate; two additional experiments gave similar results. High basal constitutive activity of ERR-γ was evaluated with the luciferase-reporter plasmid (pGL3/3 × ERRE), and the highest activity was estimated in a cell preparation of 1.0×10^5 HeLa cells/well.

Table 3. Receptor binding affinity (mean ± SE; $n = 3$) of BPA and its analogs for ER-α and their receptor selectivity for ERR-γ over ER-α.

Chemical	Binding affinity for ER-α (IC_{50}, nM)	ERR-γ receptor selectivity ER-α (IC_{50}, nM)/ERR-γ (IC_{50}, nM)
E_2	0.88 ± 0.13	Exclusively ER-α
Group A (chemicals as active as BPA for ERR-γ)		
Bisphenol E	ND	Exclusively ERR-γ
BPA	1,030 ± 146	105
4-α-Cumylphenol	4,770 ± 510	450
Group B (chemicals considerably potent for ERR-γ)		
Bisphenol B	246 ±29.7	9.46
4-*tert*-Butylphenol	ND	Exclusively ERR-γ
4-*tert*-Amylphenol	ND	Exclusively ERR-γ
4-Isopropylphenol	ND	Exclusively ERR-γ
Group C (chemicals moderately potent for ERR-γ)		
Bisphenol AP	361 ± 22.6	2.93
Bisphenol F	ND	Exclusively ERR-γ
4-*tert*-Octylphenol	925 ± 83.9	3.89
4-Ethylphenol	ND	Exclusively ERR-γ
Bisphenol AF	53.4 ± 7.28	0.15
Group D (chemicals extremely weak or inactive for ERR-γ)		
2,2-Diphenylpropane	ND	Inactive for both receptors
p-Cresol	ND	Almost inactive for both receptors
Phenol	ND	Inactive for both receptors

ND, not determined (IC_{50} value could not be calculated because of extremely weak binding activity even at a 10-μM concentration).

4-*tert*-butylphenol, 4-*tert*-amylphenol, and 4-isopropylphenol, and they were fully selective and specific for ERR-γ. In contrast, bisphenol B was very weakly active (246 nM) for ER-α, although it was still selective (about 9.5 times) for ERR-γ.

Among group C chemicals ($IC_{50}^{ERR\text{-}\gamma}$ = 120–350 nM), bisphenol F was almost completely inactive for ER-α, making it fully selective for ERR-γ (Table 3). This was also true for 4-ethylphenol. Bisphenol AP showed a weak binding affinity (361 nM) for ER-α, but it was still selective (about 3 times) for ERR-γ. However, bisphenol AF emerged as a ligand selective for ER-α with a selectivity ratio of 0.15 (Table 3). The reciprocal of 0.15 [i.e., ERR-γ (IC_{50})/ER-α (IC_{50}) = 6.67] denotes a selectivity ratio of bisphenol AF for ER-α.

The results clearly indicate that the alkyl groups on the central sp^3-C atom of bisphenol derivatives play a key role in selection of the NR ERR-γ and ER-α. When we checked the receptor binding activities of one series of bisphenol derivatives (i.e., bisphenol E, BPA, bisphenol B, bisphenol AP, and bisphenol AF), we found this line-up to be the order of compounds with increasing affinity to ER-α. At the same time, it was the order of compounds with decreasing affinity to ERR-γ. ERR-γ prefers the less bulky and less electrophilic alkyl groups, whereas ER-α appears to prefer the bulkier and more electrophilic alkyl groups.

4-*tert*-Octylphenol is a well-known endocrine disruptor candidate, but it was only moderately potent for ERR-γ (IC_{50} = 238 nM; Table 2). However, it was considerably weak for ER-α, with an IC_{50} of 925 nM; thus, we judged 4-*tert*-octylphenol to be somewhat selective (approximately 4 times) for ERR-γ. Another representative endocrine disruptor candidate is 4-nonylphenol, which was moderately active for ERR-γ (Takayanagi et al. 2006). Thus, 4-nonylphenol was slightly more selective for ERR-γ. However, some 4-alkyl phenols are distinctly more potent for ERR-γ than 4-*tert*-octylphenol and 4-nonylphenol: 4-*tert*-butylphenol, 4-*tert*-amylphenol, and 4-isopropylphenol. These 4-alkyl phenols are definitely novel candidates of the endocrine disruptor specific for ERR-γ.

Conclusion

In the present study we have shown that all the structural elements of BPA—the phenol and methyl groups and the phenyl group on the central sp^3-C atom—are prerequisite for binding to the NR ERR-γ. Furthermore, we have shown that the phenol derivatives are potent candidates for the endocrine disruptor that binds to ERR-γ. The binding affinity of [^{3}H]BPA to ERR-γ–LBD is extremely high, with a K_D value of 5.50 nM. Thus, it appears to be important to evaluate whether the previously reported effects of BPA at low doses are mediated through ERR-γ and its specific target gene(s).

At the same time, it is necessary to clarify the physiologic roles of ERR-γ and to examine the degree and ways in which BPA may influence these. This is particularly important because ERR-γ is expressed in a tissue-restricted manner—for example, it is expressed very strongly in the mammalian fetal brain and placenta—at sites that could have important outcomes for newborns. Recently, many lines of evidence have indicated that low doses of BPA affects the central nervous system (reviewed by vom Saal and Welshons 2005; Welshons et al. 2003, 2006). The molecular mechanism for these effects could involve, at least in part, the high affinity binding of BPA to ERR-γ. A similar phenomenon may be observed for other NRs, and the exploration of such chemical–receptor interactions requires a specific assay system or concept applicable to all the NRs.

References

Coward P, Lee D, Hull MV, Lehmann JM. 2001. 4-Hydroxytamoxifen binds to and deactivates the estrogen-related receptor gamma. Proc Natl Acad Sci USA 98:8880–8884.

De Lean AP, Munson PJ, Rodbard D. 1978. Simultaneous analysis of families of sigmoid dose response curves. Am J Physiol 235:E97–E105.

Dodds EC, Lawson W. 1938. Molecular structure in relation to oestrogenic activity. Compounds without a phenanthrene nucleus. Proc R Soc Lond B Biol Sci 125:222–232.

Eudy JD, Yao SF, Weston MD, Ma-Edmonds M, Talmadge CB, Cheng JJ, et al. 1998. Isolation of a gene encoding a novel member of the nuclear receptor superfamily from the critical region of Usher syndrome type IIa at 1q41. Genomics 50:382–384.

Giguère V. 2002. To ERR in the estrogen pathway. Trends Endocrinol Metab 13:220–225.

Greschik H, Flaig R, Renaud JP, Moras D. 2004. Structural basis for the deactivation of the estrogen-related receptor by diethylstilbestrol or 4-hydroxytamoxifen and determinants of selectivity. J Biol Chem 279:33639–33646.

Greschik H, Wurtz JM, Sanglier S, Bourguet W, van Dorsselaer A, Moras D, et al. 2002. Structural and functional evidence for ligand-independent transcriptional activation by the estrogen-related receptor 3. Mol Cell 9:303–313.

Gupta C. 2000. Reproductive malformation of the male offspring following maternal exposure to estrogenic chemicals. Proc Soc Exp Biol Med 224:61–68.

Heard DJ, Norby PL, Holloway J, Vissing H. 2000. Human ERRγ, a third member of the estrogen receptor-related receptor (ERR) subfamily of orphan nuclear receptors: tissue-specific isoforms are expressed during development and in the adult. Mol Endocrinol 14:382–392.

Hong H, Yang L, Stallcup MR. 1999. Hormone-independent transcriptional activation and coactivator binding by novel orphan nuclear receptor ERR3. J Biol Chem 274:22618–22626.

Horard B, Vanacker JM. 2003. Estrogen receptor-related receptors: orphan receptors desperately seeking a ligand. J Mol Endocrinol 31:349–357.

Krishnan AV, Starhis P, Permuth SF, Tokes L, Feldman D. 1993. Bisphenol-A: an estrogenic substance is released from polycarbonate flasks during autoclaving. Endocrinology 132:2279–2286.

Lorke DE, Susens U, Borgmeyer U, Hermans-Borgmeyer I. 2000. Differential expression of the estrogen receptor-related receptor gamma in the mouse brain. Brain Res Mol Brain Res 77:277–280.

Matsushima A, Kakuta Y, Teramoto T, Koshiba T, Liu X, Okada H, et al. 2007. Structural evidence for endocrine disruptor bisphenol A binding to human nuclear receptor ERRγ. J Biochem 142(4):517–524.

Nagel SC, vom Saal FS, Thayer CA, Dhar MG, Boechler M, Welshons WV. 1997. Relative binding affinity-serum modified access (RBA-SMA) assay predicts the relative *in vivo* bioactivity of the xenoestrogens bisphenol A and octylphenol. Environ Health Perspect 105:70–76.

Nakai M, Tabira Y, Asai D, Yakabe Y, Shinmyozu T, Noguchi M, et al. 1999. Binding characteristics of dialkyl phthalates for the estrogen receptor. Biophys Biochem Res Commun 254:311–314.

Olea N, Pulgar R, Pérez P, Olea-Serrano F, Rivas A, Novillo-Fertrell A, et al. 1996. Estrogenicity of resin-based composites and sealants used in dentistry. Environ Health Perspect 104:298–305.

Safe SH, Pallaroni L, Yoon K, Gaido K, Ross S, McDonnell D. 2002. Problems for risk assessment of endocrine-active estrogenic compounds. Environ Health Perspect 110(suppl 6):925–929.

Takayanagi S, Tokunaga T, Liu X, Okada H, Matsushima A, Shimohigashi Y. 2006. Endocrine disruptor bisphenol A strongly binds to human estrogen-related receptor γ (ERRγ) with high constitutive activity. Toxicol Lett 167:95–105.

vom Saal FS, Cooke PS, Buchanan DL, Palanza P, Thayer KA, Nagel SC, et al. 1998. A physiologically based approach to the study of bisphenol A and other estrogenic chemicals on the size of reproductive organs, daily sperm production, and behavior. Toxicol Ind Health 14:239–260.

vom Saal FS, Welshons WV. 2005. Large effects from small exposures. II. The importance of positive controls in low-dose research on bisphenol A. Environ Res 100:50–76.

Wang L, Zuercher WJ, Consler TG, Lambert MH, Miller AB, Orband-Miller LA, et al. 2006. X-ray crystal structures of the estrogen-related receptor-ligand binding domain in three functional states reveal the molecular basis of small molecule regulation. J Biol Chem 281:37773–37781.

Welshons WV, Nagel SC, vom Saal FS. 2006. Large effects from small exposures. III. Endocrine mechanisms mediating effects of bisphenol A at levels of human exposure. Endocrinology 147:S56–S69.

Welshons WV, Thayer KS, Judy BM, Taylor J, Curran EM, vom Saal FS. 2003. Large effects from small exposures. I. Mechanisms for endocrine-disrupting chemicals with estrogenic activity. Environ Health Perspect 111:994–1006.

Available online at www.sciencedirect.com
ScienceDirect
Bioorganic & Medicinal Chemistry
ELSEVIER
Bioorganic & Medicinal Chemistry 16 (2008) 2635–2644

Designed modification of partial agonist of ORL1 nociceptin receptor for conversion into highly potent antagonist

Jinglan Li,[a,†] Kaname Isozaki,[a,†] Kazushi Okada,[a] Ayami Matsushima,[a] Takeru Nose,[a] Tommaso Costa[b] and Yasuyuki Shimohigashi[a,*]

[a]*Laboratory of Structure–Function Biochemistry, Department of Chemistry, Research-Education Centre of Risk Science, Faculty of Sciences, Kyushu University, Fukuoka 812-8581, Japan*
[b]*Laboratorio di Farmacologia, Istituto Superiore di Sanità, Viale Regina Elena 299, Roma, Italy*

Received 6 October 2007; revised 13 November 2007; accepted 15 November 2007
Available online 21 November 2007

Abstract—Nociceptin is an endogenous agonist ligand of the ORL1 (opioid receptor-like 1) receptor, and its antagonist is a potential target of therapeutics for analgesic and antineuropathy drugs. Ac-RYYRIK-NH_2 is a hexapeptide isolated from the peptide library as an antagonist that inhibits the nociceptin activities mediated through ORL1. However, the structural elements required for this antagonist activity are still indeterminate. In the present study, we evaluated the importance of the acetyl-methyl group in receptor binding and activation, examining the peptides acyl-RYYRIK-NH_2, where acyl (R-CO) possesses a series of alkyl groups, R = C_nH_{2n+1} (n = 0–5). The isovaleryl derivative with the C_4H_9 (=$(CH_3)_2CHCH_2$–) group was found to reveal a high receptor-binding affinity and a strong antagonist nature. This peptide achieved a primary goal of eliminating the agonist activity of Ac-RYYRIK-NH_2 and producing pure antagonist activity.

1. Introduction

Nociceptin,[1] also known as orphanin FQ,[2] is a 17-mer neuropeptide with the sequence FGGFTGARKSARKLANQ. Nociceptin is an endogenous ligand of the ORL1 (opioid receptor-like 1) receptor, the structure of which is very similar to those of the δ, μ, and κ opioid receptors.[3] This receptor belongs to the G protein coupled receptor (GPCR) superfamily and couples specifically with G_i or G_o protein. Nociceptin induces hyperalgesia, and the nociceptin/ORL1 ligand–receptor system is also involved in many other physiological functions such as analgesia in the spinal cord and antiopioid effects in the brain.[1,2,4–6] The actions of nociceptin in the central nervous system also include the inhibition of locomotor activity and impairment of spatial learning.[7–9]

In general, for better understanding of such different functions of biologically active peptides, it is imperative to obtain a highly selective and specific receptor antagonist. Antagonist is an important and indispensable molecular tool for investigation of the inhibition mechanism of receptor activation. Because of the intrinsic hyperalgesic activity of nociceptin, its antagonists are expected to be highly effective analgesics.

Several different types of compounds have recently been identified as antagonists of nociceptin.[10] As full antagonists, a number of nonpeptide compounds have been designed and synthesized,[11] but it has been difficult to identify any general structural elements common to all of these organic compounds. As for compounds based on the structure of nociceptin peptide, [Phe$^1\Psi$(CH_2–NH)Gly^2]nociceptin(1–13)–NH_2[12] and [Nphe^1]nociceptin-(1–13)–NH_2[13] have been reported as antagonists in the peripheral nervous system.[14–18] However, these

Abbreviations: Boc, *tert*-butyloxycarbonyl; Bpa, *p*-benzoyl-L-phenylalanine; BSA, bovine serum albumin; DMF, *N*,*N*-dimethylformamide; GPCR, G protein coupled receptor; HBTU, 2-(1*H*-benzotriazole-1-yl)-1,1,3,3-tetramethyluronium hexafluorophosphate; HOBt, 1-hydroxybenzotriazole; MALDI–TOF, matrix-assisted laser desorption ionization time-of-flight; MBHA, *p*-methylbenzhydrylamine; Nphe, *N*-benzylglycine; RP-HPLC, reversed-phase high performance liquid chromatography; RT, retention time; TFA, trifluoroacetic acid; Tris, tris(hydroxymethyl)aminomethane.

Keywords: Acyl group; Antagonist; Nociceptin; Structure–activity relationships.

* Corresponding author. Tel./fax: +81 92 642 2584; e-mail: shimoscc@mbox.nc.kyushu-u.ac.jp
† These authors contributed equally to this study.

0968-0896/$ - see front matter © 2007 Elsevier Ltd. All rights reserved.
doi:10.1016/j.bmc.2007.11.043

peptides appear to act as partial or even full agonists of nociceptin at the central nervous site.[19–22] UFP-101, the compound with the Leu^{14} → Arg and Ala^{15} → Lys substitutions in [Nphe^{1}]nociceptin-(1–13)–NH_2, is a competitive type of nociceptin antagonist.[23] This simultaneous Leu-Ala^{14,15} → Arg-Lys substitution was reported originally by us as a structural conversion to turn nociceptin into a super agonist.[24]

In addition to these nociceptin analogues, there is another type of antagonist compound selected from the peptide libraries. For instance, acetyl-hexapeptide amide Ac-Arg-Tyr-Tyr-Arg-Ile-Lys-NH_2 (Ac-RYYRIK-NH_2) has been reported as an effective nociceptin antagonist.[25] Since Ac-RYYRIK-NH_2 displaces [^{3}H]nociceptin in a dose-dependent manner, these two peptides should share and thus compete for the binding site in ORL1 receptor. However, Ac-RYYRIK-NH_2 per se was found to exhibit partial agonist activity in the [^{35}S]GTPγS binding assay.[26,27] In addition, it did not exhibit any in vivo activity, presumably due to the rapid degradation.

Our previous study of Ala-scanning for Ac-RYYRIK-NH_2 indicated that the N-terminal tripeptide Arg-Tyr-Tyr is crucially important for binding to the ORL1 receptor.[28] In the present study, based on the fact that the analogue lacking the acetyl group, H-RYYRIK-NH_2, shows drastically reduced binding efficacy (approximately 60-fold weaker than Ac-RYYRIK-NH_2), we noted the importance of the N-terminal acetyl group, CH_3CO–, as a structural element essential for binding to ORL1.[28]

The acetyl group has two different types of structural elements—the methyl (CH_3) group and the carbonyl (CO) group. In this study, focusing on the N-terminal acetyl-methyl group, we synthesized a series of acyl-RYYRIK-NH_2 peptides (acyl = R-CO, where the alkyl group is denoted as R = C_nH_{2n+1}; n = 0–5) (Table 1), and evaluated the structural effectiveness of the acyl–alkyl group (R) for the antagonist activity. We here describe the structure–activity relationships of acyl-RYYRIK-NH_2 peptides for the best selection of ORL1 nociceptin antagonism.

2. Results

2.1. Peptide syntheses

All of the 17 N-terminal modified hexapeptides, including the parent Ac-RYYRIK-NH_2, were synthesized by the manual solid-phase method using Fmoc-amino acids. Peptides in a pure form were obtained in an average yield of approximately 31%. Among the analogues, Ada-RYYRIK-NH_2 was obtained with the best yield of approximately 56%, while *t*-BuAc-RYYRIK-NH_2 was obtained with the worst yield of less than 10% (Table 1). These were all easily soluble in water and could be assayed without any trouble. Table 1 shows the analytical data of all analogues synthesized. The purity of the peptides was verified by analytical HPLC, in which all the peptides emerged with a single peak. The retention time (approximately 34 min) of the N-terminal modified analogues is much larger than that (23.24 min) of H-RYYRIK-NH_2. It is presumed that the increased hydrophobicity of acyl groups brings about an increased retention time on HPLC. The mass numbers measured were coincident with the values calculated (data not shown). Collectively, synthetic Ac-RYYRIK-NH_2 and its analogues have been found to reveal the authentic compounds.

2.2. ORL1 receptor fused with the G protein α_o subunit for better antagonism measurement

For efficient measurements of agonism and antagonism in the receptor responses, GPCR fused with the G pro-

Table 1. Synthetic yield and HPLC analytical data of acetyl-hexapeptide amide Ac-RYYRIK-NH_2, and its analogues

n	Structure of acyl = $C_nH_{2n+1}CO$ of Acyl-RYYRIK-NH_2	Name of acyl	Abbreviations of acyl	Yield (%)	RP-HPLC retention time (min)
0	HCO–	Formyl	For	34	24.89
1	CH_3CO–	Acetyl	Ac	52	26.16
2	CH_3CH_2CO–	Propionyl	Pr	28	28.33
3	$CH_3CH_2CH_2CO$–	Butyryl	Bu	20	29.88
	$(CH_3)_2CHCO$–	Isobutyryl	isoBu	39	29.85
4	$CH_3CH_2CH_2CH_2CO$–	Valeryl	Va	21	32.94
	$(CH_3)_2CHCH_2CO$–	Isovaleryl	isoVa	14	32.35
	$CH_3CH_2CH(CH_3)CO$–	2-Methylbutanoyl	MeBut	41	31.86
	$(CH_3)_3CCO$–	Pivaloyl	Piv	23	33.25
5	$CH_3CH_2CH_2CH_2CH_2CO$–	Hexanoyl	Hex	18	35.57
	$CH_3CH_2CH_2CH(CH_3)CO$–	2-Methylpentanoyl	2-MePen	29	35.15
	$(CH_3)_3CCH_2CO$–	*tert*-Butylacetyl	*t*-BuAc	8	34.73
	$CH_3CH_2C(CH_3)_2CO$–	2,2-Dimethylbutanoyl	2,2-diMeBut	37	34.21
	$(CH_3CH_2)_2CHCO$–	2-Ethylbutanoyl	EtBut	35	34.83
	C_6H_5CO–	Benzoyl	Bz	14	36.52
	$C_{10}H_{15}CO$–	Adamantyl	Ada	56	41.89

Three of the acyl groups are not listed, since those acyl chlorides or acids are not commercially available, and thus the peptides having those acyl groups were not chemically synthesized. These include the 3-methylpentanoyl ($CH_3CH_2CH(CH_3)CH_2CO$–), 4-methylpentanoyl ($(CH_3)_2CHCH_2CH_2CO$–), and 3,3-dimethylbutanoyl ($CH_3C(CH_3)_2CH_2CO$–) groups. Elution conditions for the analytical RP-HPLC to measure the retention time: solvent system, 0.1% aqueous TFA-(A solution) and acetonitrile containing 20% A solution-(B solution) with a gradient elution from 10% to 50% B solution for 40 min; flow rate, 0.5 ml/min; temperature, 25 °C; and UV detection, 230 nm.

tein α subunit has been recognized to afford an excellent assay system.[29] In the present study, we intended to establish such a system for the ORL1 receptor. Using human ORL1 receptor, we succeeded in preparing hORL1 fused with the G protein α_o subunit (hORL1-Gα_o) for both the receptor-binding assay and the functional in vitro biological assay. We first tested this assay system for nociceptin and Ac-RYYRIK-NH_2.

For the receptor-binding assay, the highest expression efficiency of hORL1-Gα_o receptor was pursued by using COS-7 cells for the ordinary ligand-saturation experiment. Under the best conditions using the tritium-labeled ligand [^{3}H]nociceptin, the largest specific binding was obtained by subtracting its nonspecific binding from the total binding. The data were analyzed by Scatchard plot analysis, and the dissociation constant K_d was calculated to be 0.37 nM, being almost the same as the K_d value (0.41 nM) reported previously for solo rat ORL1 receptor with no G protein fused.[28] Also, in this study almost the same result (K_d = 0.40 nM) was obtained for human ORL1 receptor with no G protein fused. The results imply that both G protein fused and nonfused receptors interact with [^{3}H]nociceptin equally well.

In the ligand–receptor competitive binding assay, Ac-RYYRIK-NH_2 exhibited a very high affinity, with an IC_{50} value of 0.79 nM (Table 2). This result indicates that Ac-RYYRIK-NH_2 binds to the ORL1 receptor very strongly, and that its binding ability is almost equivalent to that of nociceptin itself (IC_{50} = 0.60 nM).

The in vitro functional activity was evaluated by measuring the fold-stimulation of [^{35}S]GTPγS binding. The activity was compared with that of nociceptin (EC_{50} = 3.91 nM) (Table 2). The extent of [^{35}S]GTPγS binding in the presence of nociceptin was at least 10 times greater than that in its absence. When the [^{35}S]GTPγS binding of the parent acetyl containing hexapeptide Ac-RYYRIK-NH_2 was measured, it was estimated to reveal approximately 60% stimulation of the maximum response by nociceptin. Obviously, Ac-RYYRIK-NH_2 is a partial agonist, and yet it possesses considerably strong agonist activity. The EC_{50} value of Ac-RYYRIK-NH_2 was estimated to be 12.9 nM, the activity of which is only approximately threefold weaker than nociceptin.

Table 2. Binding potency and biological activity of nociceptin, acetyl-hexapeptide amide Ac-RYYRIK-NH_2, and its analogues for the human ORL1 receptor fused with Gα protein

Peptides acyl-RYYRIK-NH_2 (acyl groups)	ORL1 receptor 1 binding potency IC_{50} (nM)	[^{35}S]GTPγS binding activity	
		EC_{50} (nM)	E_{max} (%)
Nociceptin	0.60 ± 0.08	3.91 ± 0.34	100
H-	218 ± 78	N.D.	—
For-	0.66 ± 0.09	23.3 ± 4.2	61 ± 2.3
Ac-	0.79 ± 0.18	12.9 ± 2.8	58 ± 3.2
Pr-	1.70 ± 0.66	27.6 ± 6.8	46 ± 3.6
Bu-	1.86 ± 0.60	32.4 ± 12.1	21 ± 3.0
isoBu-	2.81 ± 0.52	44.5 ± 11.7	14 ± 3.8
Va-	5.67 ± 0.26	N.D.	7 ± 2.1
isoVa-	7.42 ± 0.87	N.D.	≈0
MeBut-	21.3 ± 2.3	52.7 ± 16.8	27 ± 1.8
Piv-	14.9 ± 3.5	97.9 ± 20.5	32 ± 5.6
Hex-	21.7 ± 5.3	N.D.	9 ± 2.6
2-MePen-	47.3 ± 8.0	23.8 ± 4.7	17 ± 4.7
t-BuAc-	16.9 ± 4.1	46.5 ± 2.0	33 ± 2.0
2,2-diMeBut-	45.5 ± 7.1	17.7 ± 3.4	17 ± 3.4
EtBut-	92.6 ± 5.4	N.D.	10 ± 1.5
Bz-	14.7 ± 2.6	18.3 ± 4.6	38 ± 5.8
Ada-	3.42 ± 0.49	19.2 ± 5.9	35 ± 4.9

For the receptor-binding assay, [^{3}H]nociceptin was used as a tracer. Data are means ± SEM of at least three experiments (n = 3–8). N.D. (not determined) means that the activity (EC_{50} (nM)) was not calculated due to inactivity.

2.3. Activities of acyl-RYYRIK-NH_2 peptides with non-branched acyl–alkyl groups

In the binding assay using rat ORL1 receptor, the N-terminal free analogue of Ac-RYYRIK-NH_2, namely, H-RYYRIK-NH_2, exhibited a drastically diminished binding potency.[28] A similar result was obtained from the assay using the G protein-fused receptor hORL1-Gα_o. H-RYYRIK-NH_2 showed an IC_{50} value of 218 nM, indicating that it is approximately 280-fold less active than Ac-RYYRIK-NH_2 (Table 2). Since these results clearly indicate that ORL1 receptor possesses a specific binding site for the acetyl group (CH_3CO) of Ac-RYYRIK-NH_2, we attempted to optimize the acyl–alkyl group. We designed and synthesized a series of analogues, in which the acetyl group was substituted with the acyl groups (R-CO) of different alkyl groups ($R = C_nH_{2n+1}$; n = 0–5): i.e., For (n = 0, R = H), Pr (2, CH_3CH_2), Bu (3, $CH_3CH_2CH_2$), Va (4, $CH_3CH_2CH_2CH_2$), and Hex (5, $CH_3CH_2CH_2CH_2CH_2$) (Table 1).

In the ligand–receptor-binding assay, For-RYYRIK-NH_2 exhibited the highest affinity (IC_{50} = 0.66 nM) (Table 2) among all the analogues, including Ac-RYYRIK-NH_2. Since For-RYYRIK-NH_2 is almost equipotent with nociceptin (IC_{50} = 0.60 nM) in displacing [^{3}H]nociceptin, their total binding energies to attach to ORL1 must be similar to each other. As shown in Figure 1, they exhibited almost the same dose–response curves, revealing a similar binding mode. Other analogues exhibited rather weaker binding affinity as compared with the parent peptide Ac-RYYRIK-NH_2 (Table 2).

Figure 2 shows the activity profiles of nociceptin, Ac-RYYRIK-NH_2, and its analogues in the [^{35}S]GTPγS binding assay. By using the membrane preparations from the cells expressing hORL1-Gα fusion receptor, nociceptin exhibited a strong binding activity, indicating that nociceptin stimulates the G-protein activation in a dose-dependent manner. Ac-RYYRIK-NH_2 exhibited considerably high activity, and its maximum response reached 60% of that by nociceptin. For-RYYRIK-NH_2 elicited almost the same response as Ac-RYYRIK-NH_2. In contrast to their agonist activity, the maximum response of Pr-RYYRIK-NH_2 and Bu-RYYRIK-NH_2 was significantly reduced by 20% and 40%, respectively. Furthermore, it was found that Va-RYYRIK-NH_2 and Hex-RYYRIK-NH_2 were virtually devoid of agonist activity (Fig. 2). Apparently, the receptor efficacy

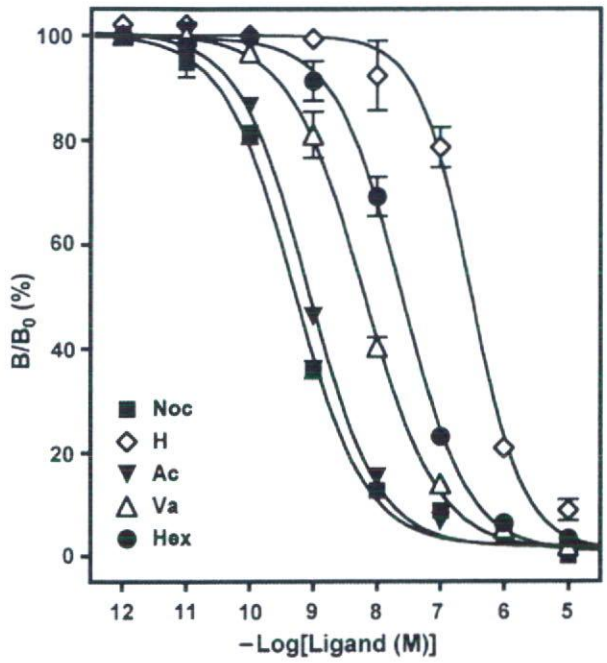

Figure 1. Dose–response curves of nociceptin and acyl-RYYRIK-NH_2 peptides in the binding assay for the hORL1-Gα fusion protein. The receptor tracer is [^{3}H]nociceptin (0.05 nM in the final concentration). The curves are of nociceptin and the parent Ac-RYYRIK-NH_2 and the analogues of acyl-RYYRIK-NH_2 with the N-terminal acyl–alkyl group R = C_nH_{2n+1}: H- (n = 0), Va- (n = 4), and Hex- (n = 5).

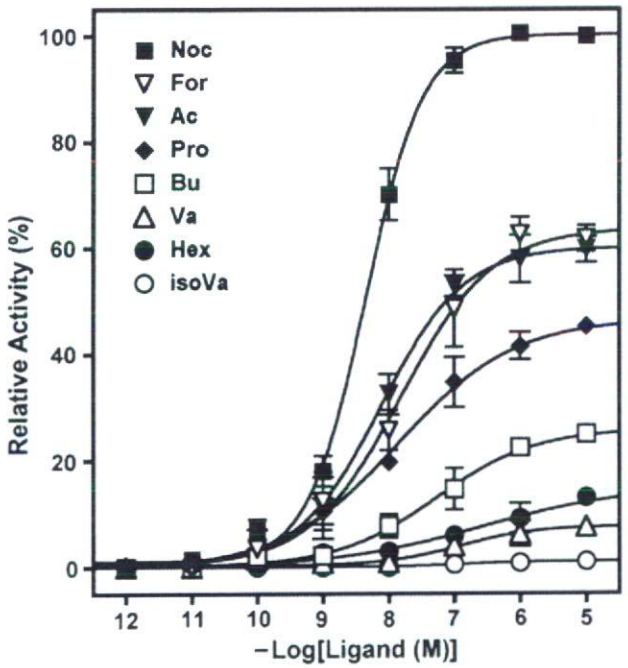

Figure 2. Dose–response curves of nociceptin and acyl-RYYRIK-NH_2 peptides in the [^{35}S]GTPγS binding assay using the hORL1-Gα receptor. Assayed acyl-RYYRIK-NH_2 peptides are with the acyl–alkyl group R = C_nH_{2n+1} (n = 0–5). Data are means ± SEM of at least five experiments.

decreased as the chain length increased. Here, it should be noted that Hex-RYYRIK-NH_2 having a hexanoyl ($CH_3CH_2CH_2CH_2CH_2CO$ = $C_5H_{11}CO$) group is clearly stronger than Va-RYYRIK-NH_2 having a valeryl ($CH_3CH_2CH_2CH_2CO$ = C_4H_9CO) group.

2.4. Activities of acyl-RYYRIK-NH_2 peptides with branched acyl–alkyl groups

In the [^{35}S]GTPγS binding assay (valeryl=)$CH_3CH_2CH_2CH_2CO$-RYYRIK-NH_2 was most active among acyl-RYYRIK-NH_2 peptides. We next examined a series of acyl-RYYRIK-NH_2, which have the acyl group (C_nH_{2n+1}-CO, n = 3–5) with eight different branched alkyl groups. Those include the acyl groups such as isobutyryl (isoBu, $(CH_3)_2CHCO$–), isovaleryl (isoVa, $(CH_3)_2CHCH_2CO$–), 2-methylbutanoyl (MeBut, $CH_3CHCH(CH_3)CO$–), pivaloyl (Piv, $(CH_3)_3CCO$–), 2-methylpentanoyl (2-MePen, $CH_3CH_2CH_2CH(CH_3)CO$–), *tert*-butylacetyl (*t*-BuAc, $(CH_3)_3CCH_2CO$–), 2,2-dimethylbutanoyl (2,2-diMeBut, $CH_3CH_2C(CH_3)_2CO$–), and 2-ethylbutanoyl (EtBut, $(CH_3CH_2)_2CHCO$–) (Table 1). The derivatives with the 3-methylpentanoyl ($CH_3CH_2CH(CH_3)CH_2CO$–) and 4-methylpentanoyl ($(CH_3)_2CHCH_2CH_2CO$–) groups were not prepared because their chlorides or acids were not commercially available. In contrast, a totally different type of acyl group, benzoyl (Bz, C_6H_5CO–) and adamantyl (Ada, $C_{10}H_{15}CO$–), was selected to assess the unique structural properties that contribute to receptor binding and activation.

When the binding ability of these acyl-substituted analogues was tested, it was found that the molecular size of the acyl–alkyl groups greatly affects the receptor-binding affinity (Table 2). The EtBut group induced the weakest activity, showing an approximately 120-fold decrease in binding affinity as compared with the parent compound Ac-RYYRIK-NH_2. Analogues having larger alkyl groups exhibited a weaker binding potency. It seems that the binding site for acyl–alkyl is not so large as to bind bulkier groups such as EtBut, 2,2-diMeBut, and 2-MePen.

Unexpectedly, the *tert*-butylacetyl (*t*-BuAc) derivative showed an affinity stronger than the compounds having acyl groups with the same molecular weight. This difference must be due to the very compact structure of the *t*-BuAc group. It was also found that Ada-RYYRIK-NH_2 is very potent (IC_{50} = 3.42 nM), despite the presence of the large acyl–alkyl $C_{10}H_{15}$. This unexpectedly high binding potency of Ada-RYYRIK-NH_2 must be due to the compactness of the adamantyl group. The π–electron rich benzoyl-protected compound Bz-RYYRIK-NH_2 also exhibits considerably strong binding potency (14.7 nM, Table 2). Collectively, the binding site for the acyl–alkyl group in the ORL-1 receptor appears to be the size of three carbons in the acyl-backone (4–5 Å) with several methyl groups.

In the [^{35}S]GTPγS binding assay, these analogues having bulky acyl groups still exhibited moderate receptor activation activity (EC_{50} = 20–50 nM and E_{max} = 10–40%, Table 2). Also, Bz-RYYRIK-NH_2 and Ada-RYYRIK-NH_2 showed an approximately 40% stimulatory response with EC_{50} of approximately 20 nM (Table 2). These results suggest that there is a space to capture

the bulky alkyl groups present at the N-terminus of R-CO-RYYRIK-NH_2, but their interaction with the ORL1 receptor is very subtle and vague, either stimulating or blocking the receptor activation.

To obstruct the receptor activation, the best-fitting alkyl group appears to be the isovaleryl (denoted as isoVa) group. The peptide isoVa-RYYRIK-NH_2 showed almost a negligible response at its 0.10–10 μM concentrations. Its E_{max} value at the 10 μM concentration was less than 5%, and thus it was impossible to estimate the EC_{50} value. It should be noted that branched isoVa-RYYRIK-NH_2 is clearly less potent than non-branched Va-RYYRIK-NH_2 in this [^{35}S]GTPγS binding assay.

2.5. Antagonist activity estimated by [^{35}S]GTPγS binding to human ORL1-Gα receptors

Because of a moderately high receptor-binding affinity (IC_{50} = 7.42 nM) and a low receptor activation efficacy, isoVa-RYYRIK-NH_2 appeared to be an efficient antagonist against nociceptin/ORL1. We then examined its competitive antagonism in the [^{35}S]GTPγS binding assay. For the Schild analysis, nociception was assayed in the presence of isoVa-RYYRIK-NH_2. Three series of dilutions of nociceptin were tested with different concentrations (10^{-8}, 10^{-7}, and 10^{-6} M concentrations, respectively) of isoVa-RYYRIK-NH_2. The assay solution was incubated for 60 min, with the expectation that competition would occur between nociceptin and isoVa-RYYRIK-NH_2 to reside in the ORL1 receptor.

As shown in Figure 3A, solo nociceptin demonstrates a superlative dose-dependent sigmoid curve. This nociceptin's concentration–response curve shifted rightward in the presence of isoVa-RYYRIK-NH_2, indicating that isoVa-RYYRIK-NH_2 occupies some population of ORL1 receptor. As the concentrations of isoVa-RYYRIK-NH_2 increased, the occupied population increased, resulting in a further rightward shift of the nociceptin curve (Fig. 3A). Eventually, the Schild analysis determined isoVa-RYYRIK-NH_2 as a potent competitive antagonist, with the pA_2 value calculated to be 8.80 (Fig. 3B). This analogue is three orders of magnitude more potent as an antagonist than [Nphe^1]nociceptin(1–13)–NH_2, and as potent as the nonpeptide J-113397,[30] the most potent antagonist reported to date.

We also examined the competitive antagonism of Va-RYYRIK-NH_2 in the [^{35}S]GTPγS binding assay. This compound shifted the nociceptin curve similar to that of isoVa-RYYRIK-NH_2, and its pA_2 value was calculated to be 8.51. Thus, together with the fact that Va-RYYRIK-NH_2 retains a weak agonist activity in the [^{35}S]GTPγS binding assay in spite of almost the complete inactivity of isoVa-RYYRIK-NH_2, we concluded that isoVa-RYYRIK-NH_2 is slightly, but definitely, more potent as an antagonist than Va-RYYRIK-NH_2 in the [^{35}S]GTPγS binding assay. As a result, the present results indicate that isoVa-RYYRIK-NH_2 is the best antagonist among the N-terminal modified hexapeptides.

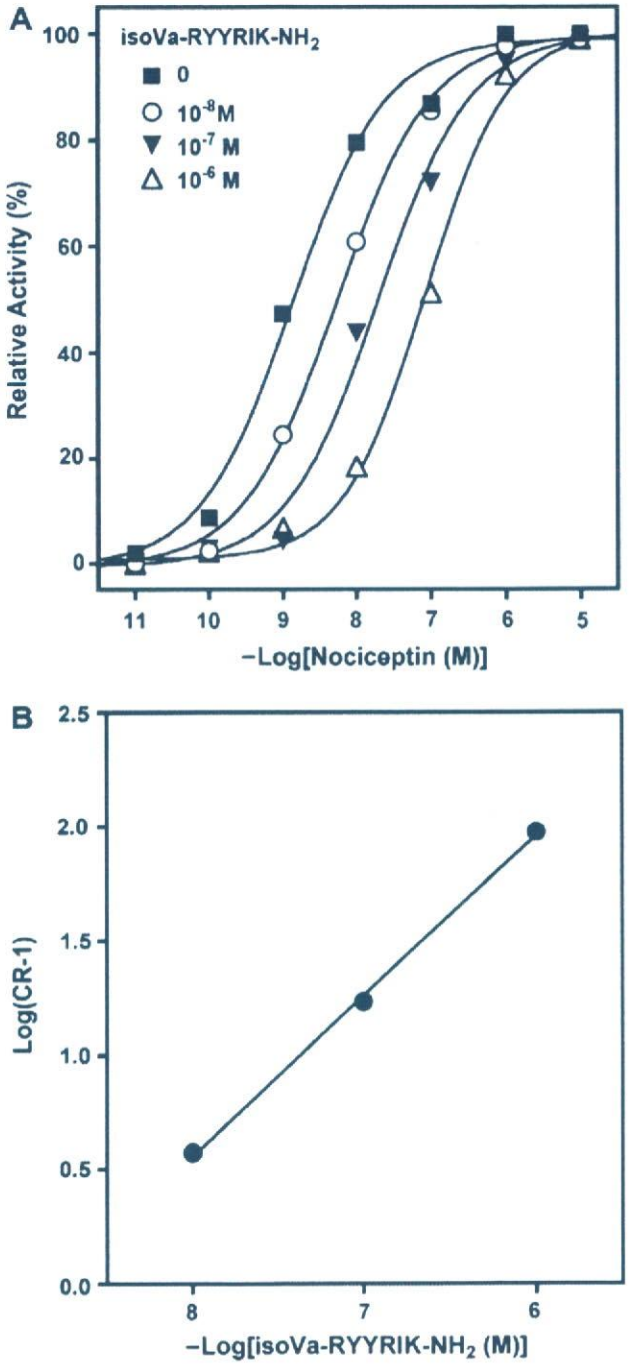

Figure 3. The antagonist activity isoVa-RYYRIK-NH_2 in the [^{35}S]GTPγS binding assay (A) and the Schild plot analysis of this assay (B). The extrapolated pA_2 value from the plot analysis was calculated to be 8.80 ± 0.20.

2.6. Antagonist activities of analogues in the mouse vas deferens

Nociceptin exerts inhibitory effects in electrically stimulated preparations such as the guinea pig ileum (GPI) and MVD.[31,32] In the present study, we established an assay system in which nociceptin inhibits the electrically evoked contractions of the MVD in a concentration-dependent manner. Its maximal effect was an approximately 80% reduction of the control contraction, and